DOI:
10.1161/JAHA.119.014811

Document Version
Peer reviewed version

Regression of atherosclerosis in ApoE-/- mice via modulation of monocyte recruitment and phenotype, induced by weekly dosing of a novel 'cytotopic' anti-thrombin without prolonged anticoagulation.

Daxin Chen MD PhD [1], Ke LI PhD[2], Sam Festenstein BSc[1], Julieta Karegli PhD[1], Hannah Wilkinson MSc MRCP[1], Hugh Leonard MRCP[1], Lin-Lin Wei MSc[2], Ning Ma MSc[2], Min Xia PhD [3], Henry Tam BSc FRCR [4], Jian-an Wang MD PhD[5], Qingbo Xu MD PhD [6], John H McVey PhD FRCPath [7], Richard AG Smith PhD[1],Anthony Dorling PhD FRCP [1]

[1]Dept. of Inflammation Biology, School of Immunology and Microbial Sciences, King's College London, Guy's Hospital, London SE1 9RT

[2]Core Research Laboratory, the Second Affiliated Hospital, School of Medicine, Jiaotong University, Xi'an 710061, China

[4]Department of Imaging, Imperial College Healthcare NHS Trust, Charing Cross Hospital, London UK.

[3]Thrombosis Research Institute, London, UK

[5]Department of Cardiology, Second Affiliated Hospital of Zhejiang University School of Medicine, Hangzhou, China

[6]Cardiovascular Division, King's College London, James Black Centre, 125 Coldharbour Lane, London SE5 9NU UK

[7]School of Bioscience & Medicine, Faculty of Health and Medical Sciences, University of Surrey, Guildford, United Kingdom.

Address for Correspondence: Anthony Dorling or Daxin Chen. MRC Centre for Transplantation, King's College London, Guy's Hospital, London SE 1 9RT. United Kingdom.

Fax: +44 207188 5660

Tel: +44 2071885880

anthony.dorling@kcl.ac.uk OR daxin.chen@kcl.ac.uk

1

Abstract:

Background: Anticoagulants induce atherosclerosis regression in animal models but exploiting this clinically is limited by bleeding events. Here we test a novel thrombin inhibitor, PTL060, comprising hirulog covalently linked to a synthetic myristoyl electrostatic switch to tether to cell membranes.

Methods and Results: ApoE-/- mice were fed chow or high fat diets, before transplantation of congenic aortic segments or injection of PTL060, parental hirulog control saline or labelled CD11b positive cells.

Aortic transplants from transgenic mice expressing anticoagulants on endothelium did not develop atherosclerosis. A single IV injection of PTL060, but not hirulog inhibited atheroma development by >50% compared to controls when assessed 4 weeks later. Mice had prolonged bleeding times for only 1/7th of the time that PTL060 was biologically active. Repeated weekly injections of PTL060 but not hirulog caused regression of atheroma. We dissected two contributory mechanisms. First, the majority of CCR2+ monocytes recruited into plaques expressed CCR7, ABCA1 and IL-10 in PTL060 mice, a phenotype seen in fewer than 20% of CCR2+ recruits in controls. Second, after several doses, there was a significant reduction in monocyte recruits, the majority of which were CCR2-negative with a similar regression-associated phenotype. Regression equivalent to that induced by IV PTL060 was induced by adoptive transfer of CD11b+ cells pre-coated with PTL060.

Conclusions: Covalent linkage of a myristoyl electrostatic switch onto hirulog in PTL060 uncouples the pharmacodynamic effects on haemostasis and atherosclerosis, such that plaque regression, mediated by predominantly via effects on monocytes, is accompanied by only transient anticoagulation.

Keywords: Atherosclerosis; Regression; Thrombin; Thrombin inhibitor

Clinical Perspective

• What is new:

• We have developed a novel direct anti-thrombin inhibitor specifically to target inflammatory processes, by covalently linking a synthetic myristoyl electrostatic switch (for cell-membrane localisation) to hirulog.

• Upon IV injection, it has the same anti-coagulant profile as equimolar hirulog, but the membrane-localising component promotes prolonged localisation on circulating leukocytes and vascular endothelium.

• This novel therapeutic induces regression of atherosclerosis in ApoE-/- mice after weekly IV dosing, by mechanisms that are dependent on this pattern of prolonged binding to cells within the vasculature,

• Throughout treatment, mice are systemically anticoagulated for only 1 day out of 7.

Clinical Implications:

• For the first time we have defined a way to uncouple the effects of hirulog on haemostasis from its effects on atheroma formation.

• Alongside our descriptions of the mechanisms through which atheroma regression is induced, our findings should provide a foundation for the development of strategies to safely harness the powerful anti-inflammatory effects of therapeutics that inhibit coagulation proteases, without adverse events related to bleeding.

Non-standard Abbreviations and Acronyms

ABCA1 - ATP-binding cassette transporter – 1
α-TFPI-Tg – a strain of transgenic mice expressing membrane tethered hTFPI under smooth muscle actin promoter
ApoE – apolipoprotein E
BL/6 – C57BL/6 mice
CCL-2 - chemokine (C-C motif) ligand 2
CCR2 - C-C chemokine receptor type 2
CCR7 - C-C chemokine receptor type 7
CD31-Hir-Tg – a strain of transgenic mice expressing membrane tethered hirudin under CD31 promoter
EC – endothelial cell
HFD – high fat diet
HLL – chemical modified hirulog
hTFPI – human tissue factor pathway inhibitor
iNOS – inducible nitric oxide synthase
LDL – low desnity lipoprotein
MIF – macrophage migration inhoibotory factor
MCSF – macrophage colony stimulating factor
ORO – Oil red O
PAR – protease activated receptor
PKH2 – green fluorescent dye taken up by phagocytic cells
PKH26 - red fluorescent dye taken up by phagocytic cells
PTL060 – the new tailed direct anti-thrombin
SMC – smooth muscle cell
TF – tissue factor

Introduction

Atherosclerosis, is a chronic inflammatory disease that causes coronary artery, peripheral vascular and cerebrovascular disease. It is a major cause of death in the Western world. Important early steps in atherogenesis, in the context of a high lipid microenvironment include secretion of chemokines such as CCL-2 and macrophage migration inhibitory factor (MIF) [1], by activated endothelial cells (ECs) and smooth muscle cells (SMCs) [2, 3] . These promote infiltration of monocytes into the subendothelial space, where they become macrophages and take up very low-density lipoprotein and low-density lipoprotein (LDL) to become foam cells, initiating the process of atheroma formation.

Coagulation proteases, such as thrombin, signal though protease activated receptors (PAR) as well as catalysing fibrin formation and are known to play a role in this process. Increased activity of tissue factor (TF), the 47-Kd cell membrane-bound glycoprotein that initiates the serine protease cascade, is seen in the neointima and underlying media of atherosclerotic plaques [4-6] and TF is expressed by EC [7], monocytes/macrophages [8] and SMC [9].

In previous work, we crossed a strain of transgenic mice expressing a membrane-tethered human Tissue Factor Pathway Inhibitor (hTFPI) fusion protein on α-smooth muscle actin (SMA)$^{+}$ cells (called α-TFPI-Tg mice) [10] with Apolipoprotein E–deficient (ApoE$^{-/-}$) mice to generate a new strain (called ApX4). These mice were resistant to atheroma formation [11]. In dissecting the mechanism of resistance, we showed that TF expression by SMC was necessary to generate MIF, via generation of thrombin and signalling primarily through PAR-1. Inhibition of either the TF, thrombin mediated PAR-1 signalling or MIF secretion prevented atherosclerosis in mice fed either a high fat diet (HFD) or a regular chow-based diet.

One of the observations from that study was that MIF continued to be secreted by EC in ApX4 mice fed a HFD, beneath which small atherosclerotic plaques developed [11]. This suggested that targeting SMC with hTFPI was not completely efficient at inhibiting atheroma.

In this new study, we explored how transgenically-expressed tethered anticoagulants on EC impacted on atherosclerosis development, and assessed the translational potential of a novel thrombin inhibitor containing the potent peptide hirulog (a direct thrombin inhibitor), that has

been chemically modified (HLL) to accept a lipid membrane-binding anchor or ‘cytotopic’ tail. This new compound is called PTL060 (thrombalexin-3). PTL060 has previously been localised within organs before transplantation to successfully inhibit thrombosis and rejection in several models [12-14]. In the process we describe an unpredicted impact of PTL060 on the phenotype of monocytes recruited into atherosclerotic plaques, by two interrelated pathways, one of which occurs by virtue of its ability to tether directly to monocytes. We also provide a mechanistic insight into the role that thrombin appears to play in driving plaque progression, as evidenced by the regression seen when PTL060 is administered systemically.

Methods

The data that support the findings of this study are available from the corresponding author upon reasonable request.

Mice and in vivo procedures

C57BL/6J (BL/6) mice were purchased from Harlan UK Ltd (Bicester, UK) and ApoE-/- mice were from the Jackson Laboratory (Bar Harbor, Maine 04609, USA). CD31-TFPI -Tg and CD31-Hir-Tg[15] mice were bred in house. Mice were housed in a temperature-controlled Specific Pathogen-Free environment at 22–24°C and all animal surgical protocols, animal experiments and care were approved by the local ethics committee and the UK Home Office. To assess the distribution of PTL060, male BL/6 mice weighing 25 – 28g (n=6 per group) were injected IV through a tail vein with either PTL060 (10µg/g in 100 µl saline), equimolar HLL (5µg/g) or saline. At 5, 30 minutes and 2, 4, 6, 24 and 48 hours mice were sacrificed to collect citrated whole blood for separation into cells and plasma and to harvest aortas for immunofluorescence analysis.

Bleeding times were assessed as previously described [15]. Briefly, mice were anesthetized and placed in a restrainer (Becton Dickinson), before a distal 3-mm segment of tail was severed with a razor blade. The tail was immediately immersed in 0.9% saline at 37°C. Bleeding time was defined as the time required for bleeding to stop. Experiments were terminated at this time or at 20 minutes.

For all atherosclerosis work, male ApoE-/- mice, from the age of 6-weeks, were fed with a HFD consisting 35 kcal% fat, 1.25% cholesterol, and 0.5% cholic acid (Special Diet Services, Essex UK). Aortas were transplanted 2 weeks after starting the HFD, using a sleeve anastomosis technique described previously [11]. Briefly, a 5mm of the segment of the infrarenal donor aorta, flushed with 300 µl of saline containing 50U of heparin, was transplanted into ApoE-/- recipient abdomen aortas (N=6 per group). Blood flow was confirmed by direct inspection after removal of the clamps. Mice were fed a HFD for 6-12 weeks post-transplantation before the experiment was terminated (Suppl fig 1A). To assess

prevention of atheroma, mice (n=6 per group) received a single injection of PTL060 or controls by tail vein, and the experiments terminated 1-3 weeks later (Suppl fig 1B). For regression experiments, baseline groups (n=6) were fed a HFD to the age of 22 weeks before the mice were sacrificed. Experimental or control groups (n=3-6 per group) received weekly injections by tail vein for 3-6 weeks, beginning at age of 22 weeks before the experiments were terminated when mice were 25-28 weeks old (Suppl fig 1C).

Cell isolation and labelling.

Leukocytes were isolated from the blood of mice aged 8-10 weeks, using anti-CD11b MicroBeads (Miltenyi Biotec Ltd, Surrey, UK) according to manufacturers' instructions. For cell labelling, $2x10^7$ CD11b+ cells were incubated with $4x10^{-6}$ M of either PKH26 or PKH2 fluorescent dyes (Sigma, UK) for 5 minutes at 25ºC according to manufacturers' protocols, with the reaction stopped using 1% BSA in PBS followed by three washes. Each recipient mouse received $0.5x10^6$ cells by IV injection; in some experiments, the cells were incubated with PTL060 (100μM in 0.5mls) or equimolar controls for 30 minutes at room temperature and washed three times before immediate injection. Cell viability was confirmed immediately prior to transfer by trypan blue extraction.

For specific viability assays, murine bone marrow cells were incubated for 5 days in 6 well plates, counted and re-seeded at $2x10^5$ cells/ml in 24 well plates with 25ng/ml MCSF. After 1 day, media was replaced with new DMEM/FCS containing different concentrations of PTL060 (or a fixed volume of control PBS), and incubated for 30-120 minutes, before assessment by flow cytometry (see below).

Histological analysis

Atherosclerotic lesions were evaluated as previously described [11]. Simply, the entire length of the aorta was perfused with PBS, dissected using a dissecting microscope, longitudinally opened and stained with Oil Red O (ORO) solution (Sigma, UK) for 30 minutes, before being photographed with a digital camera (DSC-W320, Sony, Japan). The total aortic area and

lesional area were measured by using Image J. Aortas from every animal were assessed. To assess lesions in the aortic sinus, hearts were embedded in paraffin, sectioned through the aortic root and incubated with elastin/van Gieson stain using the AccustainTM Elastin Stain kit (Sigma). Sections were examined on an Olympus U-ULH optical microscope (Olympus Optical Co. Ltd, Tokyo, Japan). Atheromatous lesional and total aortic root area was determined using Image-Pro Plus TM software version 4.0 (Media Cybernetics, Silver Spring, USA). At least three random sections were examined from each mouse in all groups. Immunohistology of frozen cross sections were prepared and examined as previously described [11]. Briefly, isolated tissues were snap-frozen and embedded in OCT compound (VWR International, Dorset, UK), sectioned at 5μm thickness and fixed in methanol at –20°C. Frozen sections were immersed in 1% bovine serum albumin–phosphate-buffered saline (BSA-PBS) for 30 minutes and then incubated overnight at 4°C with one or more of the following antibodies: rabbit polyclonal antibody to CD68, iNOs, CD206, TNFα, MIF, CCR7 ABCA1 (all from Abcam, Cambridge, UK), or hirudin (Biobyt, Cambridge, UK) or CCL2 (Lifespan BioScience, Inc., WA 98121, USA); goat polyclonal antibody to CD31 (Santa Cruz Biotechnology, Texas 75220, USA); rat anti-mouse CD68, CD11b (Serotec, Oxford, United Kingdom), CD31, IFNγ (BD Bioscience Pharmingen, Oxford, United Kingdom), Ly-6G (BioLegend, London, UK), IL-10 (Abcam) or biotinylated anti-HLL (RICS-2)[14]; mouse anti-CCR2 (Abcam). The following were used as isotype controls; goat anti-rat antibodies to IgG2a, IgG2b (BD Bioscience, Berkshire, UK) and polyclonal rabbit IgG (Abcam). The following anti-IgG FITC or TRITC-conjugated antibodies were used: sheep anti-mouse, rabbit anti-rat, goat anti-rabbit and rabbit anti-goat (all from Sigma). Fluorescein-conjugated streptavidin (Jackson Immunoresearch, Cambridge, UK) was used to detect RICS-2. Stained sections were mounted in Vectashield with DAPI (Vector Laboratories Inc, CA USA). Sections were directly captured and examined by a Leica DMIRBE confocal microscope (Leica, Wetzlar, Germany) equipped with Leica digital camera AG and a confocal laser scanning system with excitation lines at 405, 488, 543, and 560 nm at magnifications 10x/0.40CS and 20x/0.70IMM (Leica, Planapo, Wetzlar, Germany). Images were processed

using Leica-TCS-NT software associated with the Leica confocal microscope. All immunohistochemistry was performed at 22^0 C. Quantification of staining was achieved by expressing the area of positive staining as a ratio of the total lesion area, calculated using Image-Pro Plus TM, version 4.0. All quantification was performed by members of the team blinded to the identity of the sections. For estimations of positive stained area, average measurements were derived from examination of at least six random sections from each tissue sample.

To detect macrophage-derived foam cells, frozen sections of aortic sinus were analysed by a combination of ORO staining and CD68 immunostaining. Sections were incubated with rat anti-mouse CD68 antibody (overnight at 4°C) and goat anti-rat antibody (1 hour at room temperature) before staining with filtered ORO solution (0.5% in propylene glycol, Sigma) for 15 minutes at room temperature.

Plasma assays.

Anticoagulated whole blood (EDTA 30mM pH8) was separated into plasma and cells by centrifugation (14,000g for 10 mins). Plasma TNFα, IFN-γ, MIF and CCL2 were detected using separate specific ELISA kits (R&D Systems, Abingdon, UK) according to the manufacturers' instructions. Total cholesterol, high-density lipoprotein and low-density lipoprotein were determined using kits from Cell Biolabs, and Tryglycerides with a kit from Abcam, (both Cambridge, UK) according to the manufacturer's protocol. Data were derived from triplicate analysis of each sample.

Thrombin clotting times were measured in 3.2% trisodium citrated plasma according to the protocol of Ignjatovic [16]. Briefly, 100μl mouse plasma was incubated with 2.5U of human thrombin in a total volume of 300μl (Enzyme Research Laboratories (ERL), Swansea, UK) at 37°C, and the time for a clot to form was measured (n=6 per group). For some experiments plasma was further centrifuged (20,000g for 10 mins) to minimise the presence of extracellular vesicles.

Flow cytometry

The cells obtained from whole blood were washed twice in PBS with 2% FCS before staining with either anti-CD11b-FITC (Abcam) or anti-CD41-FITC (eBioscience) with biotinylated RICS2 followed by Streptavidin-PE (Bio-rad). Cells were then washed twice before analysis on a BD FACSCALIBUR with CellQuest Pro software. Erythrocytes were identified by forward/side scatter profile.

For viability assays, cells were washed twice with PBS and then incubated with Fixable LIVE/DEAD Near-IR fluorescent reactive dye (Thermofisher Scientific, Paisley, Renfrewshire, UK) for 30 minutes at 4 °C. Cells were washed, fixed for 15 minutes in 1% paraformaldehye, then washed with PBS-5% FCS and stored at 4 °C before acquisition and analysis within 24 hours on an LSRII/Fortessa flow cytometer at the BRC Flow Cytometry Laboratory, King's College London with Flowjo software (Treestar Inc). Macrophages identified by forward/side scatter profile.

SMC-MIF/CCL2 release assay *in vitro*

SMCs, cultured as previously described [11] and seeded at a density of 1×10^6 cells/well of a 24-well plate were serum-starved for 24 hours before addition of PTL060 (100μM) for 1 hour, followed by PAR agonists or antagonists (all from ERL) for 12 hours, followed by thrombin 10nM or active site inhibited thrombin (ERL) for 48 hours, before collection of supernatants. Chemokines were measured by ELISA according to the manufacturers' instructions (R&D systems, Abingdon, UK). Data were derived from triplicate analysis of each sample.

Statistical Analysis

Statistical analysis was performed with GraphPad Prism 8 software. Comparison of a single factor between two groups is by unpaired student's t test. One or Two way analysis of variances (ANOVA) was used as appropriate when making comparisons of ≥ two factors or between multiple groups. Data are presented either as mean ± SEM or as box plots with

median and interquartile range. The value of P that was considered significant was adjusted for multiple comparisons and listed in figure legends.

Results.

Anticoagulants transgenically localised to EC completely inhibit vessel wall expression of chemokines and prevent formation of atheroma.

To assess the impact of expressing hTFPI fusion protein on EC alone, we used the congenic aortic transplant model previously described [11], and compared the extent of atheroma development in transplanted aortas from CD31-TFPI-Tg mice (expressing hTFPI transgene on EC [15]) and BL/6 mice. The recipients were 8-week old ApoE-/- mice fed a HFD for 2 weeks prior to the transplant, and the experiment was terminated 6 weeks after the transplant (suppl Fig 1). In the aortic transplants from CD31-TFPI-Tg mice, MIF expression was absent through the entire wall of the transplanted vessel, not just the EC (Fig 1 A&B) and atheroma formation was significantly attenuated in the transplanted donor segment (Fig 1 F&H). In contrast and as previously reported, control BL/6 aortic transplants developed exaggerated lesions, associated with MIF expression in all layers of the vascular wall (Fig 1 E, G, H &J). The atherosclerosis that developed in the recipient aortas was independent of the type of donor aorta transplanted (Fig 1 G, H &I).

Next we transplanted aortas from a second transgenic strain (CD31-Hir-Tg) [15], expressing a tethered hirudin fusion protein on EC (suppl Fig 1), and these showed similar suppression of MIF expression throughout the vessel wall and were similarly resistant to atheroma development (Fig 1C, D, K-O), indicating that inhibition of thrombin and TF on EC was functionally equivalent, entirely consistent with our previously published results [11]. In addition to MIF, CCL-2 expression was completely suppressed throughout the vessel walls of transplants from both transgenic strains (suppl Fig 2). This data indicates that inhibiting thrombin generation (by TFPI) or the enzymatic activity of thrombin (by hirudin) on transgenic EC after transplantation into ApoE-/- mice completely suppresses MIF and CCL-2 expression throughout the entire vascular wall and prevents atheroma formation.

IV injection of PTL060, a novel tethered therapeutic anti-thrombin.

After IV administration of PTL060 into BL/6 mice, linear deposition of the anticoagulant moiety could be found on the luminal surface of the aorta mice several hours later (fig 2A). This pattern of staining was never seen after injection of parental (untailed) HLL (fig 2B). PTL060 also very quickly attached to the lipid membranes of circulating erythrocytes, leukocytes and platelets (fig 2C-E), maintaining stable levels of binding between 2-6 hours post-injection, before reducing between 24-48 hours post injection. No binding was ever seen after injection of HLL. In vitro viability assays, performed by incubating bone marrow-derived macrophages with increasing concentrations of PTL060 for 30-120 minutes confirmed no evidence of toxicity (suppl table 1).

Thrombin clotting times of citrated plasma were prolonged for > 6 hours post injection of PTL060, indicating the presence of a thrombin inhibitor, and these were not statistically different to thrombin clotting times after injection of an equimolar amount of HLL (fig 2F&G). This was associated with prolonged tail bleeding times (fig 2H) lasting for approximately 24 hours, with bleeding times in PTL060-treated mice not statistically different from those recorded in mice given an equimolar concentration of HLL (fig 2H). Thus, IV injection of PTL060 resulted in rapid uptake onto the membranes of circulating cells and platelets, with detectable deposition on EC a few hours later. Despite this, the thrombin inhibitory activity detected in plasma was indistinguishable from that seen after injection of the HLL, and mice showed prolonged bleeding for 24 hours.

We assessed the differential impact of PTL060 and HLL on expression of MIF by the vasculature, as a biomarker of potential efficacy at suppressing atheroma formation. A single IV injection of PTL060 was accompanied by complete suppression of MIF expression throughout the vessel wall for almost 1-week (suppl fig 2D; fig 3A), which was dose dependent (fig 3D). This effect was never seen in controls given saline (suppl fig 2E) or in mice administered an equimolar dose of HLL (fig 3D). This prolonged biological effect of PTL060 is consistent with our previous demonstration that, once bound to endothelium, it remains detectable for >4 days [14]. In vitro experiments confirmed that thrombin-mediated

chemokine expression was primarily via PAR-1 and that PTL060 completely inhibited this (suppl fig 3).

These data indicate that equimolar doses of PTL060 and HLL induce similar degrees of systemic thrombin inhibition lasting approximately 24 hours, but only PTL060 promotes prolonged suppression of MIF expression by vessel wall cells.

Impact of PTL060 on atherosclerosis

A single injection of PTL060 caused significant inhibition of atheroma formation in ApoE-/- mice fed a HFD for two weeks prior to, and four weeks after the injection (Fig 3A, B&C). This effect was dose dependent (fig 3D, E-H), and only occurred with doses that inhibited MIF expression for up to 1 week (fig 3A, D; suppl fig 2D). It was not seen in mice administered equimolar doses of HLL (fig 3D, H). Thus, a membrane tethered thrombin inhibitor can replicate the impact of a transgenically expressed membrane tethered thrombin inhibitor by suppressing the development of atherosclerosis.

To assess the impact of PTL060 on established atheroma, 6-week old ApoE-/- mice were fed a HFD until the age of 22 weeks, before receiving IV injections of saline, HLL, control cytotopic tail compound or PTL060, weekly for a further 6 weeks. PTL060 caused a reduction in atheroma burden, when measured either by en face analysis or by cross sectional analysis of the aortic root (fig 4A-R), an effect not seen after weekly injections of any of the controls, including HLL at equimolar doses (fig 4 A-R). This was associated with a reduction in the area of plaque occupied by lipids, as shown by Oil-red O staining (fig 4S&U), as well as a reduction in the CD68+ cells co-localising with lipid (fig 4T&U), indicating a significant reduction in the number of foam cells within the plaques. This effect of PTL060 was evident even compared to baseline mice analysed at week 16 prior to any treatment, indicating that disease regression was induced by PTL060. All the effects of PTL060 were seen without any discernible impact on body mass or circulating lipid concentrations (table 1).

PTL060 also significantly reduced atheroma burden after administration to ApoE-/- mice fed a normal chow diet, weekly from the age of 28 weeks for 6 weeks (fig 4V-Z). Under both HFD

and Chow dietary conditions, administration of PTL060 was accompanied by significant reductions in plasma levels of TNFα, IFNγ, MIF and CCL2 (suppl fig 4), compared to the appropriate controls.

The phenotype of regressing plaques after PTL060 treatment

Atheromatous plaques in ApoE-/- mice fed a HFD from 6-22 weeks of age (baseline) contained a significant number of CD68+ cells (monocytes/macrophages), occupying approximately 45% of plaque area (fig 5A,F). Compared to control animals injected with either saline or HLL (fig 5B-G), weekly injections of PTL060 reduced the proportion of plaque area occupied by CD68+ cells to below 20% (fig 5D,F) with an associated increase in the proportion of plaque cells that were CD68-negative (fig 5G). The proportion of plaque area staining for MIF reduced from >60% at baseline (fig 5A, E) to <20% (fig 5 D,E) though the proportion of CD68+ and CD68-neg cells that expressed MIF was not altered (fig 5F,G). These data indicate that PTL060 induced a shift in plaque cell composition, from predominantly CD68+ cells in control mice to predominantly CD68-negative cells after PTL060 treatment, in association with a marked reduction in vessel wall MIF expression.

Plaques developing in mice fed a HFD between 6-22 weeks were almost devoid of cells expressing the chemokine receptor CCR7 (fig 5H,K) or the cholesterol efflux regulator ATP-binding cassette transporter molecule ABCA1 (fig 5O,S), with <10% of plaque cells co-expressing these molecules (fig 5I,J & T,U). Six weeks of treatment with weekly PTL060 from weeks 22-28 caused significant increases in the proportion of plaque area occupied by cells expressing CCR7 and ABCA1 (fig 5 H,N,R,S) and almost all of these were CD68+ cells (fig 5 I,N,R,T), compared to control saline-treated mice and in contrast to mice treated with weekly injections of HLL, in whom expression of both CCR7 and ABCA1 was not statistically different to that seen at baseline (fig 5H-M & O-U).

In parallel, little IL-10 staining was seen within the plaques of any of the control animals (suppl fig 5A,B), and <2% of plaque-infiltrating CD68+ cells co-expressed IL-10 (suppl fig 5C), whereas almost all plaque infiltrating CD68+ cells expressed IFNγ (suppl fig 5E, G)) and

TNFα (suppl fig 5I,K,) and 15-20% of plaque CD68-negative cells expressed these two pro-inflammatory cytokines (supp fig 5H,L). After six weeks of PTL060, 10-15% of plaque area stained for IL-10 (suppl fig 5A, B), including 60% of the plaque-infiltrating CD68+ cells (suppl fig 5C), and approximately 10% of CD68-negative cells (suppl fig 5D). There was a marked reduction in both the proportion of plaque area (suppl fig 5E,F, I,J) and the proportion of CD68+ cells (suppl fig 5G,K) staining for INFγ and TNFα, compared to control saline-treated mice and in contrast to mice treated with weekly injections of HLL, in whom no reductions were seen. Similar dichotomous patterns of staining were seen for the macrophage polarisation markers iNOS (suppl figure 6A-D) and CD206 (suppl fig 6E-H), with staining for the former suppressed in both CD68+ and CD68-negative cells, but staining of the latter enhanced in CD68+ cells, by weekly injections of PTL060.

Thus, six weeks of weekly PTL060 injections promoted a significant reduction in plaque CD68+ cells and a significant shift in their phenotype, towards a phenotype that has previously been associated with plaque regression (CCR7+, ABCA1+, IFNγ-, IL-10+, iNOS-, CD206+).

Mechanism of regression: Impact of thrombin inhibitor tethered to the surface of circulating monocytes.

As shown already, PTL060 rapidly adheres to the surface of circulating leukocytes. To investigate the impact of this leukocyte-tethered thrombin inhibitor, in isolation to that tethered by EC or platelets and erythrocytes, we adoptively transferred CD11b+ cells labelled with the fluorescent dye PKH26 into ApoE-/- mice fed a HFD from weeks 6-22, before assessing the phenotype of the labelled plaque cells by confocal immunofluorescence microscopy 48 hours later. To avoid the potential confounding influence of transfer of PTL060 from the adoptively transferred cells to vascular membranes, for these experiments we used CD11b+ cells from CD31-Hir-Tg mice, which express covalently tethered cell surface hirudin on all monocytes, and compared the impact of labelled BL/6 cells.

At the point of adoptive transfer, MIF was expressed throughout the plaques (fig 6A), and significant numbers of labelled cells were recruited, such that they occupied 20-25% of plaque area (fig 6B, C), with no difference in the numbers of BL/6 vs CD31-Hir-Tg cells recruited (fig 6D). All recruited cells from the Tg strain expressed hirudin (fig 6C). Although the plaques already contained significant numbers of Ly6G+ granulocytes, occupying 20-25% of plaque area, and although the adoptively transferred CD11b+ populations contained granulocytes, <1% of the recruited PKH26-labelled cells co-expressed Ly6G (fig 6E-G), suggesting they were mostly monocytes, and >95% of the labelled cells, from both BL/6 and CD31-Hir-Tg, expressed CCR2 (fig 6H-J), suggesting they were predominantly Ly6Chi monocytes. Whereas none of the recruited BL/6 cells expressed ABCA1 or CCR7, the majority of CD31-Hir-Tg cells recruited to the plaques expressed both these markers (fig 6K-P). In addition, whereas the majority of recruited BL/6 cells expressed IFNγ and iNOS, these were expressed by few of the recruited CD31-Hir-Tg cells (suppl fig 7). Instead, a significant minority of these cells expressed IL-10 and CD206, markers not expressed by labelled BL/6 cells (suppl fig 7). These data illustrate that CCR2+ monocytes recruited to established plaques are polarised towards a pro-inflammatory M1 phenotype, but that a membrane tethered anti-thrombin subverts this phenotype towards one that has previously been associated with plaque regression. This strongly suggests that the shift towards regression, induced by PTL060, begins immediately post-injection via the influence of cell tethered PTL060 on the phenotype of CCR2+ monocytes recruited to existing plaques.

Monocyte recruitment and phenotype after systemic PTL060.

To assess whether PTL060 reduced numbers of monocytes recruited, ApoE-/- mice were fed a HFD from 6-22 weeks, before administration of weekly PTL060 or saline for 3 weeks to the age of 25 weeks. PKH2-labelled CD11b cells from BL/6 mice were administered one week after the last injection of PTL060 (by which time all PTL060 should have left the circulation (see Fig 2), and plaques examined 48 hours later by confocal immunofluorescence microscopy. After 3 weeks treatment with PTL060, there was significant suppression of MIF

expression by vessel wall cells (fig 7A,B), associated with a significant reduction in the number of adoptively transferred cells recruited to the plaques, such that they occupied only 2% of plaque area compared to 20% in control mice that had received saline (fig 7C).

As at baseline, the monocytes recruited into plaques of saline treated animals were predominantly CCR2+(fig 7D,F), suggesting they belonged to the Ly6Chi subset. However, monocytes recruited to plaques in PTL060-treated mice were predominantly CCR2-neg, suggesting they were predominantly Ly6Clo monocytes (fig 7E,F). Compared to cells recruited in saline treated mice, the majority of labelled cells recruited into the plaques of PTL060 mice expressed CCR7 (fig 7G-I) and ABCA1 (fig 7J-L), as well as IL-10 (suppl fig 8A-C) but fewer cells expressed TNFα (suppl fig 8D-F) or IFNγ (suppl fig 8G-I). Therefore, weekly systemic delivery of PTL060 suppressed vessel wall chemokine production, significantly reduced the recruitment of adoptively transferred monocytes by >90% compared to controls and promoted recruitment of CCR2-negative monocytes, which, independently of any direct binding of PTL060 to their cell surface, had the same phenotype that has already been associated with plaque regression.

A thrombin inhibitor on the surface of CD11b+ cells is sufficient to induce regression.

To assess whether tethering of PTL060 to leukocytes alone was sufficient to induce plaque regression, we fed ApoE-/- mice a HFD from 6-22 weeks, and then adoptively transferred, by weekly IV injection during weeks 23-28, CD11b+ cells, while continuing the HFD. Control mice received cells from BL/6 mice incubated, prior to transfer, with either saline or the cytotopic tail compound only. Experimental mice received BL/6 cells pre-incubated with PTL060 or, as a positive control, cells from CD31-Hir-Tg mice. The 30 minute incubation with these compounds had minimal effect on the viability of adoptively transferred cells (suppl table 2).

All mice receiving control cells showed progression of atherosclerosis between 23-28 weeks (fig 8A,B, E,F,I) that was not statistically different in degree to that seen in saline treated controls described earlier (see Fig 4). In contrast, mice receiving PTL060-treated BL/6 cells

(fig 8C,G,I), or cells from CD31-Hir-Tg mice (fig 8D, H, I) showed regression of plaque area not statistically different in degree to mice that had been treated with systemic PTL060 (see Fig 4). The phenotype of regressing plaques in mice given cells from CD31-Hir-Tg mice strongly resembled those in mice receiving systemic PTL060 (fig 8J).

Taken together with the data from the adoptive transfer of labelled cells, these data indicate that mechanistically, the impact of systemic PTL060 treatment can be reproduced entirely by isolating a thrombin inhibitor onto the surface of circulating monocytes, suggesting that inhibiting thrombin activity on only these cells is sufficient to promote regression.

Discussion.

The involvement of coagulation proteases in atherosclerosis and the impact of inhibiting them has been described by multiple groups in previous studies. For instance, ApoE$^{-/-}$ mice made deficient in HCII, a natural thrombin inhibitor [17], or carrying a DNA variant resulting in defective thrombomodulin-mediated generation of activated protein C [18] develop severe atheroma, indicating that in this model, endogenous regulators of thrombin act to limit disease severity. Conversely, factor (F)Xa inhibitors [19, 20] and direct thrombin inhibitors [21-24] prevent atheroma progression and maintain plaque stability Systemic anticoagulants can also induce regression of atherosclerosis in ApoE-/- mice. Bea et al used megalatran in 30-week-old animals and showed reduced burden of advanced atheromatous lesions associated with plaque stability [25]. More recently, Posthuma et al [26] reduced atheroma burden in 22 week old animals by 25% after daily treatment for 6 weeks with clinically relevant doses of the FXa inhibitor rivaroxaban.

These data from animal models have fed into clinical practice, and the benefit of systemic anticoagulation in patients with atherosclerosis has been most recently confirmed by the COMPASS trial, which showed that addition of rivaroxaban to aspirin in patients with stable atherosclerotic cardiovascular disease led to fewer deaths, strokes and myocardial infarction [27]. Moreover, the PAR-1 antagonist vorapaxar has also been shown to reduce the risk of myocardial infarction in patients with stable atherosclerosis [28]. However, these benefits were associated with a significant increase in the incidence of major bleeding events; this is the biggest drawback to using systemic anticoagulants or antiplatelet drugs for non-thrombotic diseases, as their impact on haemostasis cannot be separated from their clinical efficacy.

The development of thrombalexins built upon a foundation of tethering anti-complement compounds using a generic tail based on the myristoyl-electrostatic switch [29, 30]. We have demonstrated that several versions of thrombalexin, including PTL060 effectively bind to cell membranes, maintain potent thrombin inhibitory activity, and prevent intravascular thrombosis when infused into rodent [12] or primate kidneys [14] prior to transplantation. Under these circumstances, PTL060 remains detectable in tissue for several days.

In this work, we have shown that after IV injection, PTL060 inhibits secretion of vessel wall chemokines for 1 week and prevents atheroma formation but increases the risk of bleeding for only 24 hours. Therefore, the addition of the cytotopic tail uncouples the pharmacodynamics of hirulog's effects on haemostasis from its effects on atheroma formation, so that an increased bleeding tendency is seen for only 1/7th of the period between doses that both prevent plaque formation and induce plaque regression. To our knowledge, this is the first demonstration of such uncoupling, and represents a significant advance in understanding the true therapeutic potential of targeting coagulation proteases to influence inflammatory disease.

Our interest in this area began with the idea that targeting anticoagulants to cell membranes would achieve high concentrations in localised environments, such as the endothelium of an organ transplant, to inhibit vascular thrombosis. We demonstrated proof of concept using transgenically expressed fusion proteins [15, 31], and in the process showed that inhibiting thrombin-mediated signalling through protease activated receptors on vessels inhibited local chemokine gradients, which reduced monocyte recruitment to sites of inflammation, including after transplantation, and prolonged survival [32]. We then went on to show that thrombin was similarly involved in chemokine gradient generation in atherosclerosis, such that expression of a tethered anticoagulant on SMC significantly reduced the development of atheroma in ApoE-/- mice [11]. In this new work we have confirmed that expression of tethered anticoagulants on EC is equally efficacious at suppressing vessel wall chemokine expression by both EC and SMC in ApoE-/- mice and equally effective at preventing atherosclerosis as expression on SMC. Although there was some variation in the extent of atherosclerosis development by control ApoE-/- mice fed a HFD for 4-6 weeks across temporally distinct experiments, one consistent feature was that single doses of PTL060 caused significant inhibition (≥50%) of atheroma formation compared to controls. We have not investigated the mechanism by which targeted thrombin inhibition on EC influences the phenotype of underlying SMC, but the data are consistent with the known importance of EC / SMC

interplay for atheroma development [33], and one possibility is that it acts via regulation of angiopoietin-2 secretion, known to be important in atherosclerosis [34], which we have shown to be thrombin-dependent in a separate model system [35].

Our most important finding was that in ApoE-/- mice fed a HFD for 16 weeks prior to weekly injections of PTL060 for six weeks, atheroma burden was significantly reduced, compared not only to control mice given either saline or an equimolar dose of parental HLL, but also in comparison to baseline, indicating that PTL060 caused regression of existing disease. This was achieved without impacting plasma lipid concentrations. A similar reduction in plaque burden was seen in mice fed a normal Chow diet. There were significantly fewer CD68+ macrophages and foam cells present after 6 weeks treatment in the regressing plaques. In assessing the mechanisms of regression, we considered the importance of inhibiting vessel wall chemokine gradients. Continuous monocyte recruitment into the vessel wall is one of the major steps in the pathogenesis of atherosclerosis, as evidenced by studies showing that simultaneous inhibition of CCL2, CX3CR1 and CCR5 near abolishes development of atheroma in ApoE-/- mice [36]. In addition, deficiency of MIF also impairs atheroma development in LDL-R deficient mice [37] an inhibitory anti-MIF antibody has been shown to prevent atherosclerosis in $ApoE^{-/-}$ mice [38], and our previous work illustrated that MIF secretion was important. We confirmed that a single dose of PTL060 led to prolonged suppression of vessel wall MIF (and CCL-2), and that this associated with prevention of plaque development. In addition, recruitment of labelled CD11b+Ly6G- monocytes, adoptively transferred 1 week after the last of three doses of PTL060, was reduced by 90%, compared to that seen in control, saline-treated mice. This is consistent with the idea that suppression of vessel wall chemokine expression, interrupting the continuous cycle of monocyte recruitment, foam cell development, cell death and vessel wall inflammation might be an important contributory mechanism of how PTL060 induces plaque regression. However, PTL060 also modulated the phenotype of recruited monocytes / macrophages. Thus, plaque cells in the regressing plaques in PTL060-treated mice had a significantly

different phenotype compared to those detected in the progressing plaques in control animals, with reduced expression of pro-inflammatory IFNγ, TNFα and iNOS, and significant increases in the proportions of cells expressing CD206, IL-10, ABCA1 and CCR7.

These phenotypic characteristics have all been associated with mechanisms of regression defined in other studies. For instance after transplantation of atheromatous aorta from ApoE-/- mice into BL/6 mice [39-41], the chemokine receptor CCR7 was shown to be important for emigration of foam cells, as demonstrated by inhibiting the chemokine ligands for CCR7 [42]. In another model, LDLR-/- mice treated with an antisense to miR-33 showed regression associated with upregulated ABCA1 expression in plaque macrophages and enhanced reverse cholesterol transport [43], in association with increased levels of circulating HDL, consistent with the known importance of ABCA1 for cholesterol loading into HDL and with the phenotype of ABCA1-deficient mice [44]. Finally, the importance of polarising new monocyte recruits to the plaque towards an M2 phenotype has been recently demonstrated in the aortic transplant model, by confirming that regression is dependent on the expression of both appropriate chemokine receptors (CCR2/CX3CR1) and the transcription factor STAT6 by recipient monocytes [45].

These phenotypic changes were evident in newly recruited monocytes, but our adoptive transfer experiments suggested that CCR2+ or CCR2- monocytes were recruited at different times following PTL060 treatment. In the first experimental setting, using CD11b+ cells from CD31-Hir-Tg mice, transferred into ApoE-/- mice fed a HFD for 16 weeks without PTL060 treatment, we showed that CCR2+ monocytes were predominantly recruited, and these displayed the phenotypic traits associated with regression. In a second experimental setting, we showed that the CD11b+ cells recruited after adoptive transfer into mice already treated with 3 doses of PTL060 were predominantly CCR2- cells but also displaying the same phenotypic traits associated with regression. In this situation, labelled cells were transferred one week after the last of three doses of PTL060, into mice in which PTL060 had been cleared from the circulation, but importantly, into mice in which significant changes in plaque phenotype had already been induced. We suggest that the differential recruitment of the

CCR2- (Ly6Clo) subset, known to be precursors of M2 polarised macrophages [46], is most likely due to the conditions within the plaque already established by the PTL060. We postulate that, after the first dose, the immediate uptake of PTL060 onto the surface of circulating CCR2+ monocytes, protects them from thrombin as they are recruited into established plaques, significantly skews their phenotype as they become macrophages, and this rapidly establishes the microenvironmental conditions inside the plaque that are required to initiate regression.

Although the focus of this work has been on the impact of thrombin inhibition on the vessel wall and circulating leukocytes, they also provide a potential explanation for the mechanisms through which FXa inhibitors induce regression, though these agents would also influence signalling through PAR-2, something we've not addressed. We also showed immediate uptake of PTL060 onto circulating platelets after IV injection. Since interactions between platelets and EC and between platelets and leukocytes, via CD40, have been shown to promote leukocyte recruitment and exacerbate plaque formation in this model [47], we cannot exclude the possibility that PTL060 might be modulating these interactions.

However, the data generated showing that weekly adoptive transfer of CD11b+ cells pre-treated with PTL060, or expressing a transgenic hirudin fusion protein can induce the same degree of regression as systemic PTL060, suggests that protecting plaque-recruited monocytes from the direct effects of thrombin is the key factor required for regression. Since thrombin, via protease activated receptor-1 and cullin 3-mediated degradation is known to promote post-transcriptional downregulation of ABCA1 in macrophages [48], and is also known to promote M1 polarization of microglia after intracerebral haemorrhage [49], our data is most consistent with the hypothesis that thrombin plays a hitherto unrecognised but pivotal role in determining the inflammatory phenotype of plaque macrophages and promoting plaque progression.

Acknowledgements

We acknowledge the financial support of the King's Commercialisation Institute.

Funding Sources.

This work was funded by the Wellcome Trust (award 098300/Z/12/Z). Additional support was via the Medical Research Council (MR/P018513/1).

Disclosures.

None declared

References

1. Zernecke A, Shagdarsuren E, Weber C. Chemokines in atherosclerosis: an update. *Arterioscler Thromb Vasc Biol*. 2008;28:1897-1908
2. Hansson GK. Inflammation, atherosclerosis, and coronary artery disease. *N Engl J Med*. 2005;352:1685-1695
3. Ross R. Genetically modified mice as models of transplant atherosclerosis. *Nat Med*. 1996;2:527-528
4. Taubman MB, Fallon JT, Schecter AD, Giesen P, Mendlowitz M, Fyfe BS, Marmur JD, Nemerson Y. Tissue factor in the pathogenesis of atherosclerosis. *Thromb Haemost*. 1997;78:200-204
5. Toschi V, Gallo R, Lettino M, Fallon JT, Gertz SD, Fernandez-Ortiz A, Chesebro JH, Badimon L, Nemerson Y, Fuster V, et al. Tissue factor modulates the thrombogenicity of human atherosclerotic plaques. *Circulation*. 1997;95:594-599
6. Yamashita A, Matsuda S, Matsumoto T, Moriguchi-Goto S, Takahashi M, Sugita C, Sumi T, Imamura T, Shima M, Kitamura K, et al. Thrombin generation by intimal tissue factor contributes to thrombus formation on macrophage-rich neointima but not normal intima of hyperlipidemic rabbits. *Atherosclerosis*. 2009;206:418-426
7. Weis JR, Pitas RE, Wilson BD, Rodgers GM. Oxidized low-density lipoprotein increases cultured human endothelial cell tissue factor activity and reduces protein C activation. *FASEB J*. 1991;5:2459-2465
8. Lesnik P, Rouis M, Skarlatos S, Kruth HS, Chapman MJ. Uptake of exogenous free cholesterol induces upregulation of tissue factor expression in human monocyte-derived macrophages. *Proc Natl Acad Sci U S A*. 1992;89:10370-10374

9. Cui MZ, Penn MS, Chisolm GM. Native and oxidized low density lipoprotein induction of tissue factor gene expression in smooth muscle cells is mediated by both Egr-1 and Sp1. *J Biol Chem*. 1999;274:32795-32802

10. Chen D, Weber M, Shiels PG, Dong R, Webster Z, McVey JH, Kemball-Cook G, Tuddenham EG, Lechler RI, Dorling A. Postinjury vascular intimal hyperplasia in mice is completely inhibited by CD34+ bone marrow-derived progenitor cells expressing membrane-tethered anticoagulant fusion proteins. *J Thromb Haemost*. 2006;4:2191-2198

11. Chen D, Xia M, Hayford C, Tham EL, Semik V, Hurst S, Chen Y, Tam HH, Pan J, Wang Y, et al. Expression of human tissue factor pathway inhibitor on vascular smooth muscle cells inhibits secretion of macrophage migration inhibitory factor and attenuates atherosclerosis in ApoE-/- mice. *Circulation*. 2015;131:1350-1360

12. Karegli J, Melchionna T, Farrar CA, Greenlaw R, Smolarek D, Horsfield C, Charif R, McVey JH, Dorling A, Sacks SH, et al. Thrombalexins: Cell-Localized Inhibition of Thrombin and Its Effects in a Model of High-Risk Renal Transplantation. *Am J Transplant*. 2017;17:272-280

13. Hamaoui K, Gowers S, Boutelle M, Cook TH, Hanna G, Darzi A, Smith R, Dorling A, Papalois V. Organ Pretreatment With Cytotopic Endothelial Localizing Peptides to Ameliorate Microvascular Thrombosis and Perfusion Deficits in Ex Vivo Renal Hemoreperfusion Models. *Transplantation*. 2016;100:e128-e139

14. Manook M, Kwun J, Burghuber C, Samy K, Mulvihill M, Yoon J, Xu H, MacDonald AL, Freischlag K, Curfman V, et al. Thrombalexin: Use of a Cytotopic Anticoagulant to Reduce Thrombotic Microangiopathy in a Highly Sensitized Model of Kidney Transplantation. *Am J Transplant*. 2017;17:2055-2064

15. Chen D, Giannopoulos K, Shiels PG, Webster Z, McVey JH, Kemball-Cook G, Tuddenham E, Moore M, Lechler R, Dorling A. Inhibition of intravascular thrombosis in murine endotoxemia by targeted expression of hirudin and tissue factor pathway inhibitor analogs to activated endothelium. *Blood*. 2004;104:1344-1349
16. Ignjatovic V. Thrombin clotting time. *Methods Mol Biol*. 2013;992:131-138
17. Vicente CP, He L, Tollefsen DM. Accelerated atherogenesis and neointima formation in heparin cofactor II deficient mice. *Blood*. 2007;110:4261-4267
18. Borissoff JI, Otten JJ, Heeneman S, Leenders P, van Oerle R, Soehnlein O, Loubele ST, Hamulyak K, Hackeng TM, Daemen MJ, et al. Genetic and pharmacological modifications of thrombin formation in apolipoprotein e-deficient mice determine atherosclerosis severity and atherothrombosis onset in a neutrophil-dependent manner. *PLoS One*. 2013;8:e55784
19. Zhou Q, Bea F, Preusch M, Wang H, Isermann B, Shahzad K, Katus HA, Blessing E. Evaluation of plaque stability of advanced atherosclerotic lesions in apo E-deficient mice after treatment with the oral factor Xa inhibitor rivaroxaban. *Mediators Inflamm*. 2011;2011:432080
20. Hara T, Fukuda D, Tanaka K, Higashikuni Y, Hirata Y, Nishimoto S, Yagi S, Yamada H, Soeki T, Wakatsuki T, et al. Rivaroxaban, a novel oral anticoagulant, attenuates atherosclerotic plaque progression and destabilization in ApoE-deficient mice. *Atherosclerosis*. 2015;242:639-646
21. Lee IO, Kratz MT, Schirmer SH, Baumhakel M, Bohm M. The effects of direct thrombin inhibition with dabigatran on plaque formation and endothelial function in apolipoprotein E-deficient mice. *The Journal of pharmacology and experimental therapeutics*. 2012;343:253-257

22. Kadoglou NP, Moustardas P, Katsimpoulas M, Kapelouzou A, Kostomitsopoulos N, Schafer K, Kostakis A, Liapis CD. The beneficial effects of a direct thrombin inhibitor, dabigatran etexilate, on the development and stability of atherosclerotic lesions in apolipoprotein E-deficient mice : dabigatran etexilate and atherosclerosis. *Cardiovasc Drugs Ther*. 2012;26:367-374
23. Pingel S, Tiyerili V, Mueller J, Werner N, Nickenig G, Mueller C. Thrombin inhibition by dabigatran attenuates atherosclerosis in ApoE deficient mice. *Arch Med Sci*. 2014;10:154-160
24. Preusch MR, Ieronimakis N, Wijelath ES, Cabbage S, Ricks J, Bea F, Reyes M, van Ryn J, Rosenfeld ME. Dabigatran etexilate retards the initiation and progression of atherosclerotic lesions and inhibits the expression of oncostatin M in apolipoprotein E-deficient mice. *Drug Des Devel Ther*. 2015;9:5203-5211
25. Bea F, Kreuzer J, Preusch M, Schaab S, Isermann B, Rosenfeld ME, Katus H, Blessing E. Melagatran reduces advanced atherosclerotic lesion size and may promote plaque stability in apolipoprotein E-deficient mice. *Arterioscler Thromb Vasc Biol*. 2006;26:2787-2792
26. Posthuma JJ, Posma JJN, van Oerle R, Leenders P, van Gorp RH, Jaminon AMG, Mackman N, Heitmeier S, Schurgers LJ, Ten Cate H, et al. Targeting Coagulation Factor Xa Promotes Regression of Advanced Atherosclerosis in Apolipoprotein-E Deficient Mice. *Sci Rep*. 2019;9:3909
27. Eikelboom JW, Connolly SJ, Bosch J, Dagenais GR, Hart RG, Shestakovska O, Diaz R, Alings M, Lonn EM, Anand SS, et al. Rivaroxaban with or without Aspirin in Stable Cardiovascular Disease. *N Engl J Med*. 2017;377:1319-1330
28. Kidd SK, Bonaca MP, Braunwald E, De Ferrari GM, Lewis BS, Merlini PA, Murphy SA, Scirica BM, White HD, Morrow DA. Universal Classification System Type of

Incident Myocardial Infarction in Patients With Stable Atherosclerosis: Observations From Thrombin Receptor Antagonist in Secondary Prevention of Atherothrombotic Ischemic Events (TRA 2 degrees P)-TIMI 50. *J Am Heart Assoc*. 2016;5

29. Thelen M, Rosen A, Nairn AC, Aderem A. Regulation by phosphorylation of reversible association of a myristoylated protein kinase C substrate with the plasma membrane. *Nature*. 1991;351:320-322

30. Smith RA. Targeting anticomplement agents. *Biochem Soc Trans*. 2002;30:1037-1041

31. Chen D, Weber M, McVey JH, Kemball-Cook G, Tuddenham EG, Lechler RI, Dorling A. Complete inhibition of acute humoral rejection using regulated expression of membrane-tethered anticoagulants on xenograft endothelium. *Am J Transplant*. 2004;4:1958-1963

32. Chen D, Carpenter A, Abrahams J, Chambers RC, Lechler RI, McVey JH, Dorling A. Protease-activated receptor 1 activation is necessary for monocyte chemoattractant protein 1-dependent leukocyte recruitment in vivo. *J Exp Med*. 2008;205:1739-1746

33. Li M, Qian M, Kyler K, Xu J. Endothelial-Vascular Smooth Muscle Cells Interactions in Atherosclerosis. *Front Cardiovasc Med*. 2018;5:151

34. Yu H, Moran CS, Trollope AF, Woodward L, Kinobe R, Rush CM, Golledge J. Angiopoietin-2 attenuates angiotensin II-induced aortic aneurysm and atherosclerosis in apolipoprotein E-deficient mice. *Sci Rep*. 2016;6:35190

35. Chen D, Li K, Tham EL, Wei LL, Ma N, Dodd PC, Luo Y, Kirchhofer D, McVey JH, Dorling A. Inhibition of Angiopoietin-2 Production by Myofibrocytes Inhibits

Neointimal Hyperplasia After Endoluminal Injury in Mice. *Frontiers in immunology*. 2018;9:1517

36. Combadiere C, Potteaux S, Rodero M, Simon T, Pezard A, Esposito B, Merval R, Proudfoot A, Tedgui A, Mallat Z. Combined inhibition of CCL2, CX3CR1, and CCR5 abrogates Ly6C(hi) and Ly6C(lo) monocytosis and almost abolishes atherosclerosis in hypercholesterolemic mice. *Circulation*. 2008;117:1649-1657

37. Pan JH, Sukhova GK, Yang JT, Wang B, Xie T, Fu H, Zhang Y, Satoskar AR, David JR, Metz CN, et al. Macrophage migration inhibitory factor deficiency impairs atherosclerosis in low-density lipoprotein receptor-deficient mice. *Circulation*. 2004;109:3149-3153

38. Burger-Kentischer A, Gobel H, Kleemann R, Zernecke A, Bucala R, Leng L, Finkelmeier D, Geiger G, Schaefer HE, Schober A, et al. Reduction of the aortic inflammatory response in spontaneous atherosclerosis by blockade of macrophage migration inhibitory factor (MIF). *Atherosclerosis*. 2006;184:28-38

39. Feig JE. Regression of atherosclerosis: insights from animal and clinical studies. *Ann Glob Health*. 2014;80:13-23

40. Fisher EA. Regression of Atherosclerosis: The Journey From the Liver to the Plaque and Back. *Arterioscler Thromb Vasc Biol*. 2016;36:226-235

41. Moore KJ, Sheedy FJ, Fisher EA. Macrophages in atherosclerosis: a dynamic balance. *Nat Rev Immunol*. 2013;13:709-721

42. Trogan E, Feig JE, Dogan S, Rothblat GH, Angeli V, Tacke F, Randolph GJ, Fisher EA. Gene expression changes in foam cells and the role of chemokine receptor CCR7 during atherosclerosis regression in ApoE-deficient mice. *Proc Natl Acad Sci U S A*. 2006;103:3781-3786

43. Rayner KJ, Sheedy FJ, Esau CC, Hussain FN, Temel RE, Parathath S, van Gils JM, Rayner AJ, Chang AN, Suarez Y, et al. Antagonism of miR-33 in mice promotes reverse cholesterol transport and regression of atherosclerosis. *J Clin Invest*. 2011;121:2921-2931

44. Aiello RJ, Brees D, Francone OL. ABCA1-deficient mice: insights into the role of monocyte lipid efflux in HDL formation and inflammation. *Arterioscler Thromb Vasc Biol*. 2003;23:972-980

45. Rahman K, Vengrenyuk Y, Ramsey SA, Vila NR, Girgis NM, Liu J, Gusarova V, Gromada J, Weinstock A, Moore KJ, et al. Inflammatory Ly6Chi monocytes and their conversion to M2 macrophages drive atherosclerosis regression. *J Clin Invest*. 2017;127:2904-2915

46. Woollard KJ, Geissmann F. Monocytes in atherosclerosis: subsets and functions. *Nat Rev Cardiol*. 2010;7:77-86

47. Gerdes N, Seijkens T, Lievens D, Kuijpers MJ, Winkels H, Projahn D, Hartwig H, Beckers L, Megens RT, Boon L, et al. Platelet CD40 Exacerbates Atherosclerosis by Transcellular Activation of Endothelial Cells and Leukocytes. *Arterioscler Thromb Vasc Biol*. 2016;36:482-490

48. Raghavan S, Singh NK, Mani AM, Rao GN. Protease-activated receptor 1 inhibits cholesterol efflux and promotes atherogenesis via cullin 3-mediated degradation of the ABCA1 transporter. *J Biol Chem*. 2018;293:10574-10589

49. Wan S, Cheng Y, Jin H, Guo D, Hua Y, Keep RF, Xi G. Microglia Activation and Polarization After Intracerebral Hemorrhage in Mice: the Role of Protease-Activated Receptor-1. *Transl Stroke Res*. 2016;7:478-487

Table 1: Effect of PTL060 on body mass and plasma lipids in ApoE-/- mice

Prevention experiments		Aortic Tx recipients*- fed HFD 6-14 weeks (n=6 per group)						Single injection* – fed HFD 6-12 weeks (n=6 per group)					
		BL/6	CD31-TFPI-Tg	P value∆	BL/6	CD31-Hlr-Tg	P value∆	PBS	HLL (5μg/g)	PTL060 (2.5μg/g)	PTL060 (5μg/g)	PTL060 (10μg/g)	P value†
Body mass	Age 6 weeks	18.6±0.27	18.6±0.25	0.99	19.6±0.42	19.6±0.31	0.99	19.0±0.40	19.4±0.22	19.4±0.44	19.4±0.38	19.2±0.24	0.87
	End of Exp.	25.2±1.71	24.6±1.36	0.63	26.8±0.34	25.9±0.77	0.99	32.0±1.63	32.0±0.99	31.4±0.84	29.8±0.35	29.4±0.73	0.36
Cholesterol (mmol/L)		53.1±3.31	52.9±3.67	0.99	50.1±4.98	50.2±5.77	0.99	51.0±5.56	54.1±5.70	49.3±4.56	50.3±4.36	50.1±5.44	0.97
Triglycerides (mmol/L)		2.1±0.14	2.0±0.20	0.99	2.0±0.13	2.0±0.14	0.99	2.1±0.31	2.1±0.36	2.2±0.28	2.2±0.27	2.1±0.30	1.00
HDL(mmol/L)		1.5±0.11	1.5±0.10	0.99	1.6±0.07	1.5±0.08	0.99	1.4±0.28	1.5±0.08	1.6±0.12	1.5±0.09	1.5±0.09	0.92
LDL (mmol/L)		57.2±2.73	55.2±3.49	0.97	63.9±9.97	61.0±6.28	0.92	55.6±6.64	54.7±4.48	54.1±4.72	51.7±5.89	52.8±5.42	0.99
Regression experiments			Series 1 HFD 6-28 weeks (n=6 per group)					Series 2 HFD 6-28 weeks (n=6 per group)					
		6-week old	Baseline⌀	PBS¥	Tail only	PTL060 (10μg/g)	P value†	Baseline⌀	PBS	HLL (5μg/g)	PTL060 (5μg/g)	PTL060 (10μg/g)	P value†
Body mass	Age 6 weeks	-	19.3±0.28	19.6±0.37	19.1±0.15	19.3±0.38	0.74	20.2±0.39	20.1±0.38	20.6±0.07	20.1±0.30	20.3±0.26	0.73
	Age 22 weeks	-	30.5±0.58	32.8±0.44	30.4±0.90	32.0±0.81	0.19	31.5±1.34	31.4±0.84	31.1±0.66	31.2±1.00	31.9±0.78	0.85
	End of Exp.	-	-	33.2±0.31	31.8±0.73	28.7±1.55	0.03	-	32.9±1.19	31.4±0.33	30.2±0.93	29.8±0.59	0.11
Cholesterol (mmol/L)		10.3±4.6	56.7±6.08	61.5±6.51	61.9±6.35	57.9±3.61	0.88	54.9±6.25	56.9±6.93	54.1±5.39	53.9±6.31	54.3±13.1	0.41
Triglycerides (mmol/L)		0.36±0.14	2.08±0.15	2.25±0.11	2.49±0.13	2.19±0.16	0.26	2.27±0.28	1.68±0.31	2.21±0.38	2.2±0.33	2.16±0.69	0.86
HDL(mmol/L)		4.46±1.1	1.54±0.007	1.49±0.06	1.46±0.06	1.56±0.06	0.65	1.61±0.12	1.58±0.11	1.78±0.2	1.6±0.16	1.68±0.38	0.27
LDL (mmol/L)		14.4±2.8	46.5±3.39	56.1±2.92	57.4±2.57	50.8±2.84	0.07	53.8±3.51	62.7±4.43	63.5±3.55	60.6±6.79	63.3±16.7	0.97

HFD; high fat diet. BL/6; C57BL/6J. HLL; hirulog modified to accept the myristoyl tail (NB: HLL 5μg is equimolar to PTL060 10μg). PBS; phosphate buffered saline. Exp.; experiment. HDL; high density lipoprotein. LDL; low density lipoprotein.
'n' refers to number of animals per group. Samples from each animal were analysed in triplicate.
*In prevention experiments, aortic transplants performed and single injections given to mice aged 8 weeks, 2 weeks after starting HFD.
⌀Baseline = week 22. Mice in the 'baseline' groups were harvested at this timepoint prior to any treatment
¥Treatments given weekly by IV injection for 6 weeks (mice aged 22-28 weeks).
∆ Two way ANOVA for multiple groups
† One way ANOVA for multiple groups (NB: values from 6-week old mice not included in comparisons)

Figure Legends:

Figure 1: Inhibition of TF or thrombin on EC abolishes MIF expression in vascular wall and prevents formation of atheroma.

A-E. Three colour immunofluorescence images of sections through donor aortas, 6-12 weeks post-transplantation. Recipients were ApoE-/- mice, fed a high fat diet (HFD) for two weeks from age 6 weeks, prior to transplantation of aorta from CD31-TFPI-Tg (A,B), CD31-Hir-Tg (C-D) or C57BL/6 mice (E). Blue - nuclear stain 4',6-diamidino-2-phenylindole (DAPI). Red - anti-hTFPI (A,B), anti-hirudin (Hir-C,D) or anti-CD31 (E). Green - MIF (A,C,E) or CD31 (B,D). Each panel of three images shows consecutive sections.

F-J – Analysis of atheroma development in whole aorta (F,G,H) and aortic root (H,I,J) after a HFD for 6 weeks post-transplantation. F&G: representative Oil Red O-stained en face preparations of aorta from ApoE-/- mice transplanted with aorta from CD31-TFPI-Tg (F) or BL/6 (G) mice. The transplanted section is highlighted by arrows. H: Quantitative assessments show the area occupied by atheroma, assessed at three different sites (as indicated) as a proportion of the total area (n=6 males each group) in ApoE-/- mice transplanted with aortas from CD31-TFPI-Tg (white bars) or BL/6 (grey bars) donors. Graphs show box plots with median with interquartile range (IQR) with whiskers showing upper and lower limits and outliers indicated as single data points. Means are represented with 'x'. I&J Representative light photomicrographs of elastic/van Gieson stained sections from aortic root of mice transplanted with aortas from CD31-TFPI-Tg (I) or BL/6 (J) mice.

K-O – Analysis of atheroma development in the whole aorta (K, L,M) and aortic root (M, N, O) after a HFD for 12 weeks post-transplantation. K&L: representative Oil Red O-stained en face preparations of aorta from ApoE-/- mice transplanted with aorta from CD31-Hir-Tg (K) or BL/6 (L) mice. The transplanted section is highlighted by arrows. M: Quantitative assessments show the area occupied by atheroma, assessed at three different sites (as indicated) as a proportion of the total area (n=6 males each group) in ApoE-/- mice transplanted with aortas from CD31-Hir-Tg (white bars) or BL/6 (grey bars) donors. Graphs

show box plots with median with interquartile range (IQR) with whiskers showing upper and lower limits and outliers indicated as single data points. Means are represented with 'x'. N&O representative light photomicrographs of elastic/van Gieson stained sections from aortic root of mice transplanted with aortas from CD31-Hir-Tg (N) or BL/6 (O) mice. Quantitative analyses were performed by a member of the team blinded to the mouse strain. Comparisons of plaque development analysed by repeated measures two way Anova. Because multiple comparisons were made from these animals, $p<0.02$ is statistically significant.

Figure 2: Impact of IV PTL060.

A&B: Two colour IF images of cross sections through aorta harvested at 6 hours post-IV injection of 10μg/g PTL060 (A) or equimolar (5μg/g) HLL (B) stained with isotype control or RICS2 antibody (which recognises HLL) as indicated. Blue -DAPI. (NB Sections examined at all other time points showed less evidence of binding by PTL060).

C-E: Flow cytometric assessment of binding to erythrocytes (C), CD11b+ leukocytes (D) and platelets (gated on CD41+) (E) obtained from mice given either saline control, HLL (2.5μg/g), or PTL060 (5μg/g). Graphs show percentage of population binding RICS antibody (left column) and the geometric mean of the fluorescence intensity of binding (right column). Samples were taken from mice at the time points post-injection as indicated. n=3 per group.

F&G: Thrombin clotting times (seconds ± SEM) in plasma. Blood was collected into citrated tubes at the times specified under terminal anaesthesia before spinning at 15000g for 10 minutes to separate out cellular components and plasma. Thrombin times performed by adding 25U (F) or 50U (G) thrombin to 100 μl of plasma and recording time for a fibrin clot to form. Mice (n=3 per group) injected with PTL060 (5μg/g – filled squares) or equimolar dose of HLL (2.5μg/g – circles). Plasma from mice treated with PTL060 was centrifuged for a further 20 minutes at 10000g, to remove any membrane bound PTL060, before repeating assessments (open squares).

H: Graph depicting tail bleeding times in minutes ± SEM at various times after IV injection of control phosphate buffered saline (open circles), PTL060 10μg/g (squares) or equimolar (5μg/g) HLL (closed circles). N=6 per group. Mouse euthanised at 20 minutes if tail still bleeding.

Figure 3: IV PTL060 inhibits MIF and prevents atherosclerosis

A: Quantitative impact of PTL060 on MIF expression by endothelium (left axis), represented as the proportion of CD31+ cells staining for MIF, plotted against time or development of atheroma (right axis) 4 weeks post injection. Mice (n=6) given either PBS control (white) or PTL060 10μg/g (grey) by IV injection, 2 weeks after starting a HFD and analysed at the time points indicated. Graphs show box plots with median with interquartile range (IQR) with whiskers showing upper and lower limits and outliers indicated as single data points. Means are represented with 'x'. Comparisons of plaque development analysed by unpaired t test. $P<0.05$ is statistically significant.

B&C: Representative light photomicrographs of elastic/van Gieson stained sections from aortic root of ApoE-/- mice treated with PBS (B) or 10μg/g PTL060 (C).

D: Quantitative impact of PTL060 on MIF expression 1-week post injection (left axis), represented as the proportion of CD31+ cells staining for MIF, or development of atheroma (right axis) 4 weeks post injection. Mice (n=6) given either PTL060 2.5μg/g (white bars), PTL060 5μg/g (grey bars), PTL060 10μg/g (striped bars) or HLL 5μg/g (diamond bars) by IV injection, 2 weeks after starting a HFD and analysed at the time points indicated. HLL 5μg/g is equimolar to PTL060 10μg/g. Graphs show box plots with median with interquartile range (IQR) with whiskers showing upper and lower limits and outliers indicated as single data points. Means are represented with 'x'. Comparisons of plaque development analysed by repeated measures one-way Anova. $P<0.05$ is statistically significant

E-H: Representative light photomicrographs of elastic/van Gieson stained sections from aortic root of ApoE-/- mice treated with PTL060 2.5μg/g (E), 5μg/g (F), 10μg/g (G), or HLL 5μg/g (H).

Figure 4: IV PTL060 causes regression of atherosclerosis

A-D: Representative Oil Red O-stained en face preparations of aorta from ApoE-/- mice fed a HFD from age of 6-22 weeks (baseline: A), or 6-28 weeks with weekly injections (weeks 23-28) of saline (B), control cytotopic 'tail' compound (C) or PTL060 10μg/g (D).

E-H: Representative light photomicrographs of elastic/van Gieson stained sections from aortic root of ApoE-/- mice fed a HFD from age of 6-22 weeks (baseline: E), or 6-28 weeks with weekly injections (weeks 23-28) of saline (F), control cytotopic 'tail' compound (G) or PTL060 10μg/g (E).

I: Quantitative comparison of impact of PTL060 on atheroma formation in mice on HFD aged 6-22 weeks (white bars) or 6-28 weeks with weekly injections (weeks 23-28) of saline (grey bars), control 'tail' compound (striped bars) or PTL060 10μg/g (diamond bars). Comparisons of plaque development analysed by repeated measures two-way Anova. Because multiple comparisons were made from these animals, $p<0.008$ is statistically significant.

J-M: Representative Oil Red O-stained en face preparations of aorta from ApoE-/- mice fed a HFD from age of 6-22 weeks (Baseline: J), or 6-28 weeks with weekly injections (weeks 23-28) of saline (K), control 'untailed' HLL (L) or PTL060 10μg/g (M).

N-Q: Representative light photomicrographs of elastic/van Gieson stained sections from aortic root of ApoE-/- mice fed a HFD from age of 6-22 weeks (N), or 6-28 weeks with weekly injections (weeks 23-28) of saline (O), control untailed HLL (P) or PTL060 10μg/g (Q).

R: Quantlitative comparison of impact of PTL060 on atheroma formation in mice on HFD aged 6-22 weeks (white bars) followed by weekly injections, for 6 weeks of saline (grey bars), control untailed HLL (striped bars) or PTL060 10μg/g (diamond bars). Comparisons of

plaque development analysed by repeated measures two way Anova. Because multiple comparisons were made from these animals, $p<0.0026$ is statistically significant.

S-T: Impact of PTL060 on foam cells in atherosclerosis. Representative light photomicrographs of elastic/van Gieson stained sections from aortic root (S) with consecutive sections analysed by two-colour immunofluorescence (T) stained with DAPI (blue) or anti-CD68 (green). ApoE-/- mice were fed a HFD from age of 6-22 weeks, followed by weekly injections, for 6 weeks of saline, control untailed HLL or PTL060 10μg/g as indicated.

U: Graphical representations of the % of plaque area staining with Oil Red O (upper panel) and, in lower panel, the % of area occupied by CD68+ cells (white bars) with the proportion of those CD68+ cells co-localising with lipid (grey bars). Each graph is a box plot with median with interquartile range (IQR) with whiskers showing upper and lower limits and outliers indicated as single data points. Means are represented with 'x'. Data is derived from an assessment of each of the three aortic root plaques from 6 individual mice, from consecutive sections as illustrated in S&T. Comparisons of plaque development analysed by repeated measures two-way Anova. Because multiple comparisons were made from these animals, $p<0.0026$ is statistically significant.

V-W: Representative Oil Red O-stained en face preparations of aorta from ApoE-/- mice fed a normal chow diet to the age of 28 weeks, followed by weekly injections, for 6 weeks of saline (V) or PTL060 10μg/g (W).

X-Y: Representative light photomicrographs of elastic/van Gieson stained sections from aortic root of ApoE-/- mice fed a chow diet age to the age of 28 weeks, followed by weekly injections, for 6 weeks of saline (X) or PTL060 10μg/g (Y).

Z: Quantitative comparison of impact of PTL060 on atheroma formation in mice on chow diet to for 28 weeks followed by weekly injections, for 6 weeks of saline (white bars) or PTL060 10μg/g (grey bars). Comparisons of plaque development analysed by two way Anova. $P<0.05$ is statistically significant.

Figure 5: Phenotype of plaque cells after PTL060

Three colour immunofluorescence images show confocal microscopic analysis of consecutive sections of aortic roots of ApoE-/- mice, fed a high fat diet from 6 to 22 weeks ('Baseline' A, K,O) or 6-28 weeks, with mice administered weekly injections of saline (B,L,P), HLL (C,M,Q), or PTL060 (D,N,R) as indicated between weeks 22-28. Panels show the plaque expression of CD68 (red) with (green) either MIF (A-D) CCR7 (K-N) or ABCA1 (O-R). Yellow in overlay image indicates co-localisation. The plaque area is demarcated by the lumen (L) and the dotted white line. Le= aortic leaflet.

Each panel of images is accompanied by graphical representations of the % of plaque area staining for the molecule of interest (E-MIF, H-CCR7, S-ABCA1) and the % of plaque area occupied by CD68+ (F, I, T) and the proportion of CD68+ cells (white bars) and CD68-negative cells (grey bars) co-staining for MIF (G), CCR7 (J), or ABCA1 (U). Each graph is a box plot with median with interquartile range (IQR) with whiskers showing upper and lower limits and outliers indicated as single data points. Means are represented with 'x'. Each is derived from an assessment of each of the three aortic root plaques from 6-24 individual mice.

Comparisons of plaque composition analysed by repeated measures two-way Anova. Because multiple comparisons were made from these animals, $p<0.0026$ is statistically significant.

Figure 6 – Impact of adoptive transfer of CD11b+ cells expressing tethered thrombin inhibitor

All panels: CD11b cells, harvested from either BL/6 or CD31-Hir-Tg mice were labelled in vitro with PKH26 (red) and adoptively transferred into ApoE-/- mice fed a HFD between ages of 6-22 weeks. Aortic roots were collected 48 hours post-injection, for confocal IF analysis of the phenotype of adoptively transferred cells. Graphs are a box plot with median with interquartile range (IQR) with whiskers showing upper and lower limits and outliers indicated

as single data points. Means are represented with ‘x’. Each is derived from an assessment of at least 3 aortic root plaques from 6-35 individual mice.

A: To illustrate the expression of MIF (green) at baseline age 22 weeks, throughout the plaque area in a mouse that received BL/6 CD11b+ cells.

B-D: Comparison of the recruitment of CD11b+ cells from BL/6 (B) and CD31-Hir-Tg (C) mice. Hirudin (green) only seen in cells from CD31-Hir-Tg mice. D illustrates quantitative assessment of the proportion of plaque area occupied by PKH26+ cells.

E-G: To illustrate expression of Ly6G (green) within the plaque after adoptive transfer of CD11b+ cells from BL/6 (E) or CD31-HIr-Tg (F) mice. G illustrates quantitative assessment of the proportion of PKH26+ cells co-expressing Ly6G.

I-J: To illustrate expression of CCR2 (green) within the plaque after adoptive transfer of CD11b+ cells from BL/6 (H) or CD31-HIr-Tg (I) mice. J illustrates quantitative assessment of the proportion of PKH26+ cells co-expressing CCR2.

K-M: To illustrate expression of ABCA1 (green) within the plaque after adoptive transfer of CD11b+ cells from BL/6 (K) or CD31-HIr-Tg (L) mice. M illustrates quantitative assessment of the proportion of PKH26+ cells co-expressing ABCA1.

N-P: To illustrate expression of CCR7 (green) within the plaque after adoptive transfer of CD11b+ cells from BL/6 (N) or CD31-HIr-Tg (O) mice. P illustrates quantitative assessment of the proportion of PKH26+ cells co-expressing CCR7.

Quantitative comparisons analysed by repeated measures two-way Anova. Because multiple comparisons were made from these animals, $p<0.0055$ is statistically significant.

Figure 7: Monocyte recruitment and phenotype after systemic PTL060.

Confocal microscopic analysis of three colour immunofluorescence images through consecutive sections of aortic roots of ApoE-/- mice, fed a high fat diet from 6 to 26 weeks, with mice administered weekly injections of saline or PTL060 as indicated below between weeks 22-25. 1 week after the last injection, mice were injected with PKH2-labelled CD11b

cells (green) and aortic roots harvested 48 hours later. Graphs are a box plot with median with interquartile range (IQR) with whiskers showing upper and lower limits and outliers indicated as single data points. Means are represented with 'x'. Each is derived from a double assessment of each of the three aortic root plaques from 3 individual mice.

A-C: To illustrate the expression of MIF (red) after adoptive transfer of BL/6 CD11b+ cells in mice treated with saline (A) or PTL060 (B). C illustrates quantitative assessment of the proportion of plaque area occupied by PKH2+ cells.

D-F: To illustrate the expression of CCR2 (red) after adoptive transfer of BL/6 CD11b+ cells in mice treated with saline (D) or PTL060 (E). F illustrates quantitative assessment of the proportion of PKH2+ cells co-expressing CCR2.

G-I: To illustrate the expression of CCR7 (red) after adoptive transfer of BL/6 CD11b+ cells in mice treated with saline (G) or PTL060 (H). I illustrates quantitative assessment of the proportion of PKH2+ cells co-expressing CCR7.

J-K: To illustrate the expression of ABCA1 (red) after adoptive transfer of BL/6 CD11b+ cells in mice treated with saline (J) or PTL060 (K). L illustrates quantitative assessment of the proportion of PKH2+ cells co-expressing ABCA1.

Quantitative comparisons analysed by repeated measures two-way Anova. Because multiple comparisons were made from these animals, $p<0.007$ is statistically significant

Figure 8: *Regression induced by thrombin inhibitor on isolated CD11b+ cells*

Samples represented here are from ApoE-/- mice fed a HFD from age of 6-28 weeks with weekly (weeks 23-28) injections of CD11b+ cells from BL/6 mice pre-incubated with saline (A, E), control 'tail' molecule (B, F), PTL060 100μM (C,G) or with CD11b cells from CD31-Hir-Tg mice (D, H)

A-D: Representative Oil Red O-stained en face preparations of aorta

E-H: Representative light photomicrographs of elastic/van Gieson stained sections from aortic root

I: Quantitative comparison of atheroma regression in the whole aorta (en face) or aortic root of mice fed a HFD from age of 6-28 weeks with weekly (weeks 23-28) injections of CD11b+ cells from BL/6 mice pre-incubated with saline (white bars), control 'tail' molecule (grey bars), PTL060 100μM (striped bars) or with CD11b cells from CD31-Hir-Tg mice (diamond bars). J: Graph is a box plot with median with interquartile range (IQR) with whiskers showing upper and lower limits and outliers indicated as single data points. Means are represented with 'x'. Each is derived from an assessment of at least 3 aortic root plaques from 6-24 individual mice. It illustrates the proportion of plaque area occupied by cells expressing the various markers (as indicated on abscissa) from mice receiving CD11b+ cells from BL/6 mice pre-incubated with saline (white bars) or CD31-Hir-Tg mice (grey bars).

Quantitative comparisons in I&J analysed by repeated measures two-way Anova. Because multiple comparisons were made from these animals, $p<0.0055$ is statistically significant.

Supplementary Figure Legends

Suppl Figure 1: Illustration of th in vivo models used in this manuscript. A: aortic transplantation. B: prevention of atherosclerosis. C: Regression of atherosclerosis.

Suppl Figure 2: Inhibition of TF or thrombin on EC abolishes CCL2 and MIF expression in vascular walls

A-C. Three colour immunofluorescence images of sections through donor aortas, 6 weeks post-transplantation. Recipients were ApoE-/- mice, fed a high fat diet (HFD) for two weeks from age 6 weeks, prior to transplantation of aorta from BL/6 (A) CD31-TFPI-Tg (B) or CD31-Hir-Tg (C). Blue - nuclear stain 4',6-diamidino-2-phenylindole (DAPI). Red - anti-CD31 (A) anti-hTFPI (B) or anti-hirudin (Hir-C). Green – CCL2. Each panel of three images shows consecutive sections.

D&E: Three colour IF images of consecutive sections through aortic root, taken 1, 2 or 3 weeks post IV injection of 10μg/g of PTL060 (D) or PBS (E). $ApoE^{-/-}$ mice were commenced on a high fat diet 2 weeks prior to the injections. Blue - DAPI. Red - anti-CD31. Green - MIF.

Suppl Figure 3: PTL060 inhibits thrombin- and PAR-1-mediated chemokine production in vitro.

In vitro analysis of MIF (A) or CCL2 (B) production by cultured mouse SMCs, following stimulation by thrombin, with addition of reagents to demonstrate that PTL060 predominantly inhibits PAR-1 mediated chemokine production.

Comparisons of significance by unpaired 2-tailed students t test. $P<0.05$ is considered significant.

Experiment repeated twice.

Suppl Figure 4: Systemic inhibition of inflammation by PTL060.

Plasma TNFα (A), IFNγ (B), MIF (C) and CCL2 (D) in different groups of ApoE-/- mice, as indicated on abscissa.

Graphs show box plots with median with interquartile range (IQR) with whiskers showing upper and lower limits and outliers indicated as single data points. Means are represented with 'x'. Comparisons analysed by repeated measures two way Anova. Because multiple comparisons were made from these animals, $p<0.0026$ is statistically significant.

Suppl Figure 5: Phenotype of plaque cells induced by PTL060_2

Confocal microscopic analysis of three colour immunofluorescence images through consecutive sections of aortic roots of ApoE-/- mice, fed a high fat diet from 6 to 22 weeks ('Baseline', all panels) or 6-28 weeks, with mice administered weekly injections of saline, HLL, or PTL060 as indicated between weeks 22-28. Panels show the plaque expression of CD68 (red) with (green) either IL-10 (A) IFNγ (E) or TNFα (I). Yellow in overlay image indicates co-localisation. The plaque area is demarcated by the lumen (L) and the dotted white line. Le= aortic leaflet.

Each panel of images is accompanied by graphical representations of the % of plaque area staining for the molecule of interest (B-IL-10, F-IFNγ, J-TNFα) and the % of plaque area occupied by CD68+ (C, G, K) and the proportion of CD68+ cells (white bars) and CD68-negative cells (grey bars) co-staining for IL-10 (D), IFNγ (H), or TNFα (L). Each graph is a box plot with median with interquartile range (IQR) with whiskers showing upper and lower limits and outliers indicated as single data points. Means are represented with 'x'. Each is derived from an assessment of each of the three aortic root plaques from at least 6 individual mice. Comparisons analysed by repeated measures two-way Anova. Because multiple comparisons were made from these animals, $p<0.0026$ is statistically significant.

Suppl Figure 6: Phenotype of plaque cells induced by PTL060_3

Confocal microscopic analysis of three colour immunofluorescence images through consecutive sections of aortic roots of ApoE-/- mice, fed a high fat diet from 6 to 22 weeks ('Baseline', all panels) or 6-28 weeks, with mice administered weekly injections of saline, HLL, or PTL060 as indicated between weeks 22-28. Panels show the plaque expression of CD68 (red) with (green) either iNOs (A) or CD206 (E). Yellow in overlay image indicates co-localisation. The plaque area is demarcated by the lumen (L) and the dotted white line. Le= aortic leaflet.

Each panel of images is accompanied by graphical representations of the % of plaque area staining for the molecule of interest (B-iNOS, F-CD206) and the % of plaque area occupied by CD68+ (C, G) and the proportion of CD68+ cells (white bars) and CD68-negative cells (grey bars) co-staining for iNOS (D) or CD206 (H). Each graph is a box plot with median with interquartile range (IQR) with whiskers showing upper and lower limits and outliers indicated as single data points. Means are represented with 'x'. Each is derived from an assessment of each of the three aortic root plaques from at least 6 individual mice. Comparisons analysed by repeated measures two-way Anova. Because multiple comparisons were made from these animals, $p<0.0026$ is statistically significant.

Suppl Figure 7 – Impact of adoptive transfer of CD11b+ cells expressing hirudin_2

All panels: CD11b cells, harvested from either BL/6 or CD31-Hir-Tg mice were labelled in vitro with PKH26 (red) and adoptively transferred into ApoE-/- mice fed a HFD between ages of 6-22 weeks. Aortic roots were collected 48 hours post-injection, for confocal IF analysis of the phenotype of adoptively transferred cells. Graphs are a box plot with median with interquartile range (IQR) with whiskers showing upper and lower limits and outliers indicated as single data points. Means are represented with 'x'. Each is derived from a double assessment of each of the six aortic root plaques from 6 individual mice.

A-C: To illustrate expression of IFNγ (green) within the plaque after adoptive transfer of CD11b+ cells from BL/6 (A) or CD31-HIr-Tg (B) mice. C illustrates quantitative assessment of the proportion of PKH26+ cells co-expressing IFNγ.

D-F: To illustrate expression of IL-10 (green) within the plaque after adoptive transfer of CD11b+ cells from BL/6 (D) or CD31-HIr-Tg (E) mice. F illustrates quantitative assessment of the proportion of PKH26+ cells co-expressing IL-10.

G-I: To illustrate expression of iNOS (green) within the plaque after adoptive transfer of CD11b+ cells from BL/6 (G) or CD31-HIr-Tg (H) mice. I illustrates quantitative assessment of the proportion of PKH26+ cells co-expressing iNOS.

J-L: To illustrate expression of CD206 (green) within the plaque after adoptive transfer of CD11b+ cells from BL/6 (J) or CD31-HIr-Tg (K) mice. L illustrates quantitative assessment of the proportion of PKH26+ cells co-expressing CD206.

Quantitative comparisons analysed by repeated measures two-way Anova. Because multiple comparisons were made from these animals, $p<0.0055$ is statistically significant.

Suppl Figure 8: Monocyte recruitment and phenotype after systemic PTL060_2.

Confocal microscopic analysis of three colour immunofluorescence images through consecutive sections of aortic roots of ApoE-/- mice, fed a high fat diet from 6 to 26 weeks, with mice administered weekly injections of saline or PTL060 as indicated below between weeks 22-25. 1 week after the last injection, mice were injected with PKH2-labelled CD11b cells (green) and aortic roots harvested 48 hours later. Graphs are a box plot with median with interquartile range (IQR) with whiskers showing upper and lower limits and outliers indicated as single data points. Means are represented with ‘x’. Each is derived from a double assessment of each of the three aortic root plaques from 3 individual mice.

A-C: To illustrate the expression of IL-10 (red) at adoptive transfer of BL/6 CD11b+ cells in mice treated with saline (A) or PTL060 (B). C illustrates quantitative assessment of the proportion of PKH2+ cells co-expressing IL-10.

D-F: To illustrate the expression of TNFα (red) at adoptive transfer of BL/6 CD11b+ cells in mice treated with saline (D) or PTL060 (E). F illustrates quantitative assessment of the proportion of PKH2+ cells co-expressing TNFα.

G-I: To illustrate the expression of IFNγ (red) at adoptive transfer of BL/6 CD11b+ cells in mice treated with saline (G) or PTL060 (H). I illustrates quantitative assessment of the proportion of PKH2+ cells co-expressing IFNγ.

Quantitative comparisons analysed by repeated measures two-way Anova. Because multiple comparisons were made from these animals, $p<0.007$ is statistically significant.

Figure 1

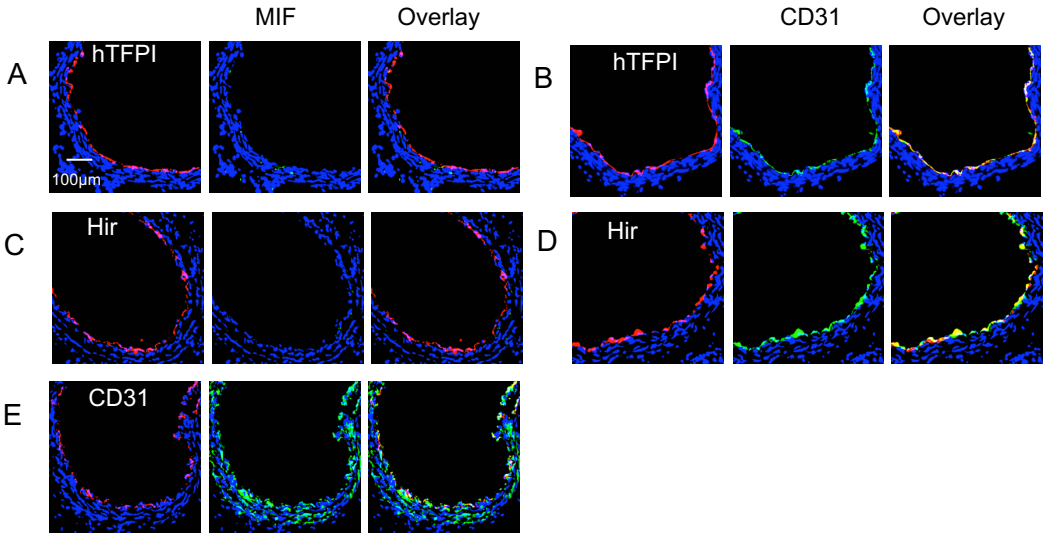
MIF
Overlay
CD31
Overlay
A
hTFPI
100µm
B
hTFPI
C
Hir
D
Hir
E
CD31

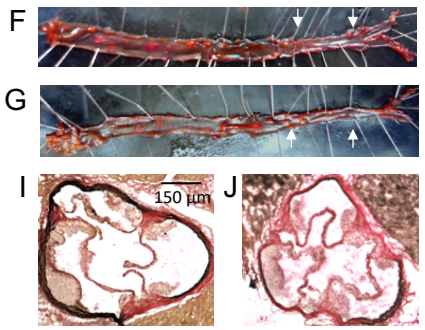
F
G
I
150 µm
J

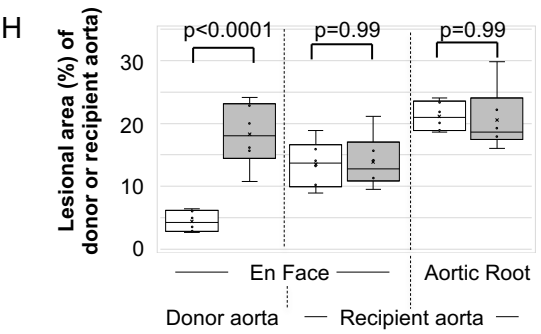
H
Lesional area (%) of donor or recipient aorta)
p<0.0001
p=0.99
p=0.99
30
20
10
0
En Face
Aortic Root
Donor aorta
Recipient aorta

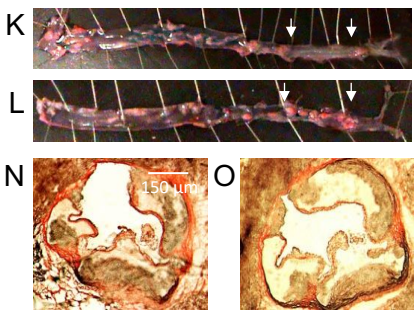
K
L
N
150 µm
O

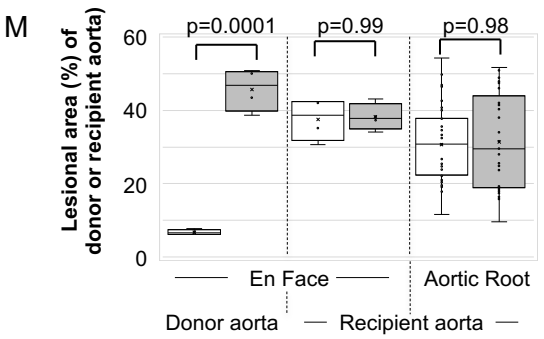
M
Lesional area (%) of donor or recipient aorta)
p=0.0001
p=0.99
p=0.98
60
40
20
0
En Face
Aortic Root
Donor aorta
Recipient aorta

Figure 1: Inhibition of TF or thrombin on EC abolishes MIF expression in vascular wall and prevents formation of atheroma.

A-E. Three colour immunofluorescence images of sections through donor aortas, 6-12 weeks post-transplantation. Recipients were ApoE-/- mice, fed a high fat diet (HFD) for two weeks from age 6 weeks, prior to transplantation of aorta from CD31-TFPI-Tg (A,B), CD31-Hir-Tg (C-D) or C57BL/6 mice (E). Blue - nuclear stain 4',6-diamidino-2-phenylindole (DAPI). Red - anti-hTFPI (A,B), anti-hirudin (Hir-C,D) or anti-CD31 (E). Green - MIF (A,C,E) or CD31 (B,D). Each panel of three images shows consecutive sections.

F-J – Analysis of atheroma development in whole aorta (F,G,H) and aortic root (H,I,J) after a HFD for 6 weeks post-transplantation. F&G: representative Oil Red O-stained en face preparations of aorta from ApoE-/- mice transplanted with aorta from CD31-TFPI-Tg (F) or BL/6 (G) mice. The transplanted section is highlighted by arrows. H: Quantitative assessments show the area occupied by atheroma, assessed at three different sites (as indicated) as a proportion of the total area (n=6 males each group) in ApoE-/- mice transplanted with aortas from CD31-TFPI-Tg (white bars) or BL/6 (grey bars) donors. Graphs show box plots with median with interquartile range (IQR) with whiskers showing upper and lower limits and outliers indicated as single data points. Means are represented with 'x'. I&J Representative light photomicrographs of elastic/van Gieson stained sections from aortic root of mice transplanted with aortas from CD31-TFPI-Tg (I) or BL/6 (J) mice.

K-O – Analysis of atheroma development in the whole aorta (K, L,M) and aortic root (M, N, O) after a HFD for 12 weeks post-transplantation. K&L: representative Oil Red O-stained en face preparations of aorta from ApoE-/- mice transplanted with aorta from CD31-Hir-Tg (K) or BL/6 (L) mice. The transplanted section is highlighted by arrows. M: Quantitative assessments show the area occupied by atheroma, assessed at three different sites (as indicated) as a proportion of the total area (n=6 males each group) in ApoE-/- mice transplanted with aortas from CD31-Hir-Tg (white bars) or BL/6 (grey bars) donors. Graphs show box plots with median with interquartile range (IQR) with whiskers showing upper and lower limits and outliers indicated as single data points. Means are represented with 'x'. N&O representative light photomicrographs of elastic/van Gieson stained sections from aortic root of mice transplanted with aortas from CD31-Hir-Tg (N) or BL/6 (O) mice.

Quantitative analyses were performed by a member of the team blinded to the mouse strain. Comparisons of plaque development analysed by repeated measures two way Anova. Because multiple comparisons were made from these animals, $p<0.02$ is statistically significant.

Figure 2

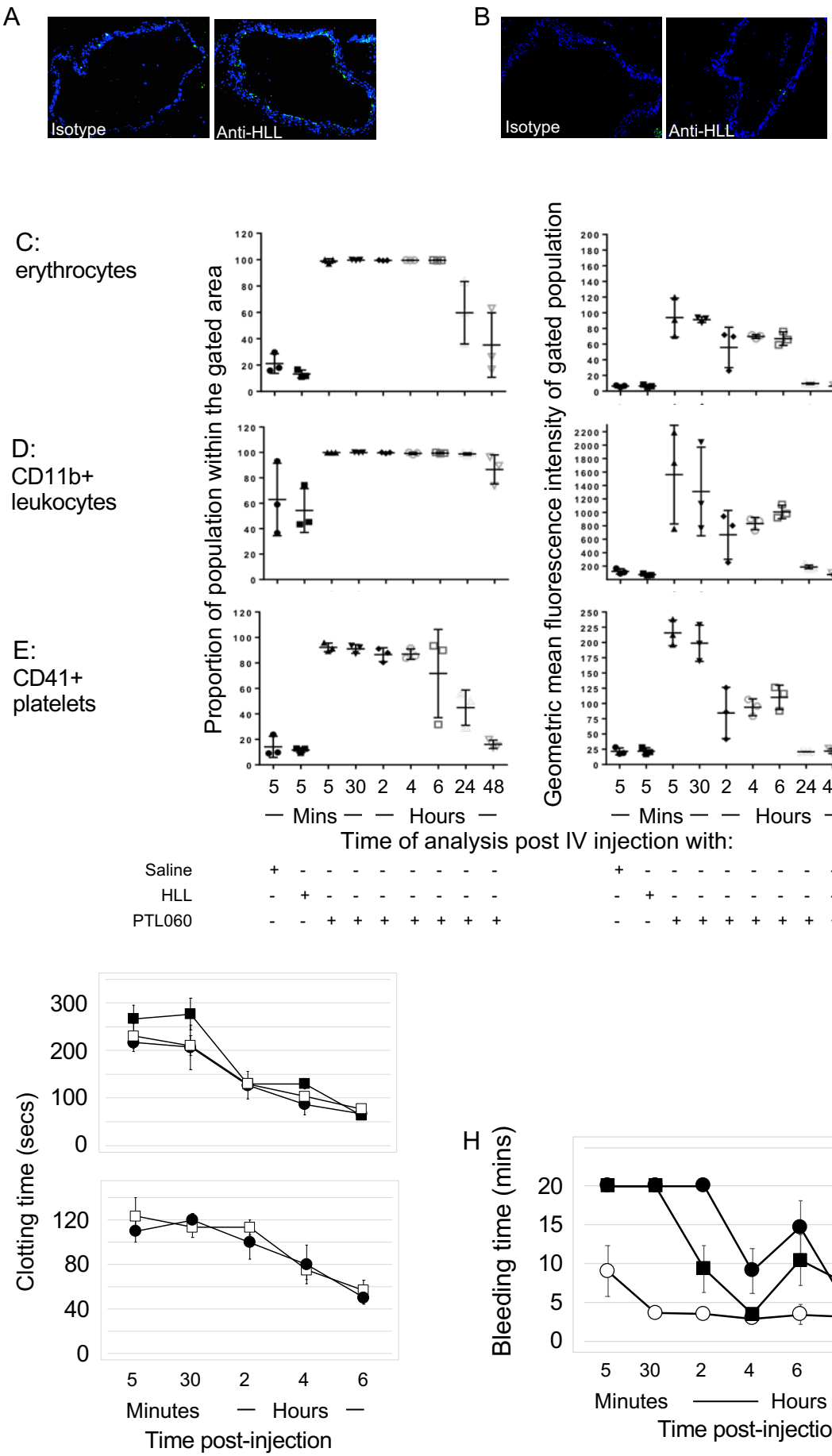
A
Isotype
Anti-HLL
B
Isotype
Anti-HLL
C:
erythrocytes
D:
CD11b+
leukocytes
E:
CD41+
platelets
Proportion of population within the gated area
Geometric mean fluorescence intensity of gated population
5 5 5 30 2 4 6 24 48
Mins
Hours
Time of analysis post IV injection with:
Saline
HLL
PTL060
F
Clotting time (secs)
G
Minutes
Hours
Time post-injection
H
Bleeding time (mins)
5 30 2 4 6 24 48
Minutes
Hours
Time post-injection

Figure 2: Impact of IV PTL060.

A&B: Two colour IF images of cross sections through aorta harvested at 6 hours post-IV injection of 10μg/g PTL060 (A) or equimolar (5μg/g) HLL (B) stained with isotype control or RICS2 antibody (which recognises HLL) as indicated. Blue -DAPI. (NB Sections examined at all other time points showed less evidence of binding by PTL060).

C-E: Flow cytometric assessment of binding to erythrocytes (C), CD11b+ leukocytes (D) and platelets (gated on CD41+) (E) obtained from mice given either saline control, HLL (2.5μg/g), or PTL060 (5μg/g). Graphs show percentage of population binding RICS antibody (left column) and the geometric mean of the fluorescence intensity of binding (right column). Samples were taken from mice at the time points post-injection as indicated. n=3 per group.

F&G: Thrombin clotting times (seconds ± SEM) in plasma. Blood was collected into citrated tubes at the times specified under terminal anaesthesia before spinning at 15000g for 10 minutes to separate out cellular components and plasma. Thrombin times performed by adding 25U (F) or 50U (G) thrombin to 100 μl of plasma and recording time for a fibrin clot to form. Mice (n=3 per group) injected with PTL060 (5μg/g – filled squares) or equimolar dose of HLL (2.5μg/g – circles). Plasma from mice treated with PTL060 was centrifuged for a further 20 minutes at 10000g, to remove any membrane bound PTL060, before repeating assessments (open squares). n=3 per group.

H: Graph depicting tail bleeding times in minutes ± SEM at various times after IV injection of control phosphate buffered saline (open circles), PTL060 10μg/g (squares) or equimolar (5μg/g) HLL (closed circles). N=6 per group. Mouse euthanised at 20 minutes if tail still bleeding.

Figure 3

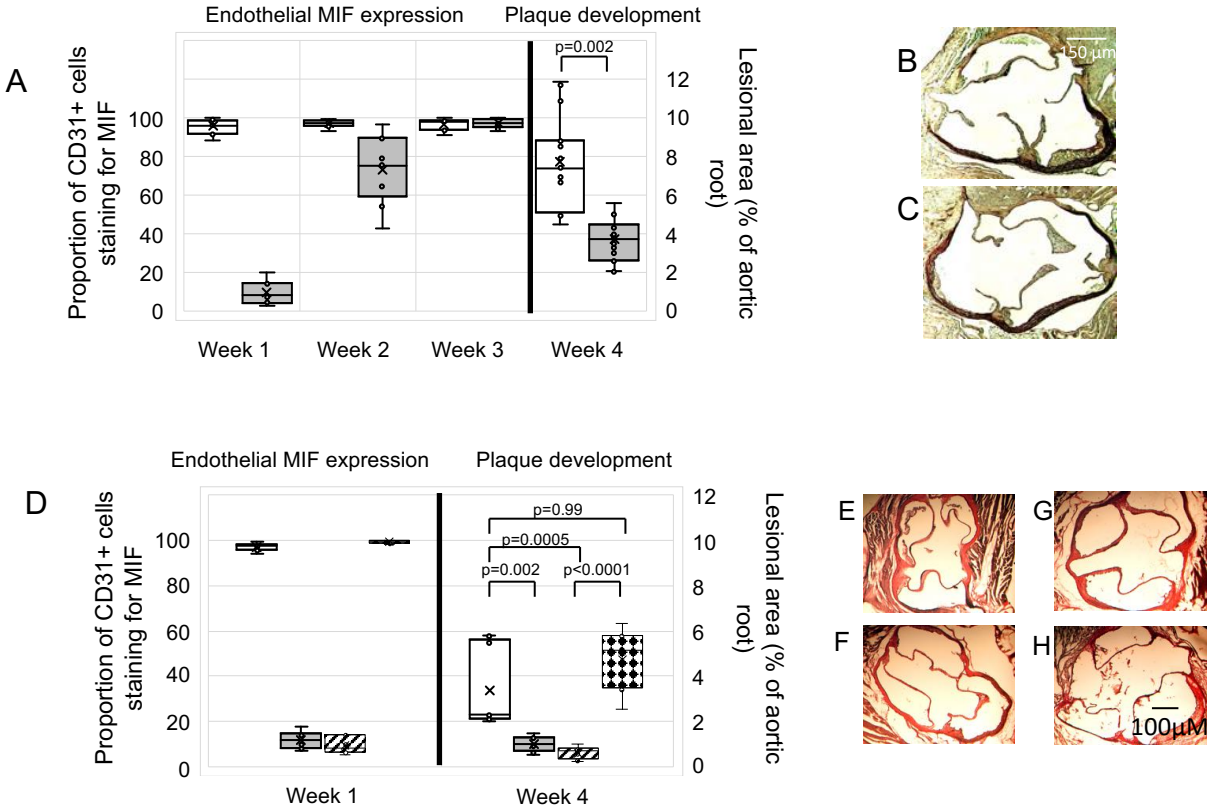

Figure 3: IV PTL060 inhibits MIF and prevents atherosclerosis

A: Quantitative impact of PTL060 on MIF expression by endothelium (left axis), represented as the proportion of CD31+ cells staining for MIF, plotted against time or development of atheroma (right axis) 4 weeks post injection. Mice (n=6) given either PBS control (white) or PTL060 10µg/g (grey) by IV injection, 2 weeks after starting a HFD and analysed at the time points indicated. Graphs show box plots with median with interquartile range (IQR) with whiskers showing upper and lower limits and outliers indicated as single data points. Means are represented with 'x'. Comparisons of plaque development analysed by unpaired t test. $P<0.05$ is statistically significant.

B&C: Representative light photomicrographs of elastic/van Gieson stained sections from aortic root of ApoE-/- mice treated with PBS (B) or 10µg/g PTL060 (C).

D: Quantitative impact of PTL060 on MIF expression 1-week post injection (left axis), represented as the proportion of CD31+ cells staining for MIF, or development of atheroma (right axis) 4 weeks post injection. Mice (n=6) given either PTL060 2.5µg/g (white bars), PTL060 5µg/g (grey bars), PTL060 10µg/g (striped bars) or HLL 5µg/g (diamond bars) by IV injection, 2 weeks after starting a HFD and analysed at the time points indicated. HLL 5µg/g is equimolar to PTL060 10µg/g. Graphs show box plots with median with interquartile range (IQR) with whiskers showing upper and lower limits and outliers indicated as single data points. Means are represented with 'x'. Comparisons of plaque development analysed by repeated measures one-way Anova. $P<0.05$ is statistically significant.

E-H: Representative light photomicrographs of elastic/van Gieson stained sections from aortic root of ApoE-/- mice treated with PTL060 2.5µg/g (E), 5µg/g (F), 10µg/g (G), or HLL 5µg/g (H).

Figure 4

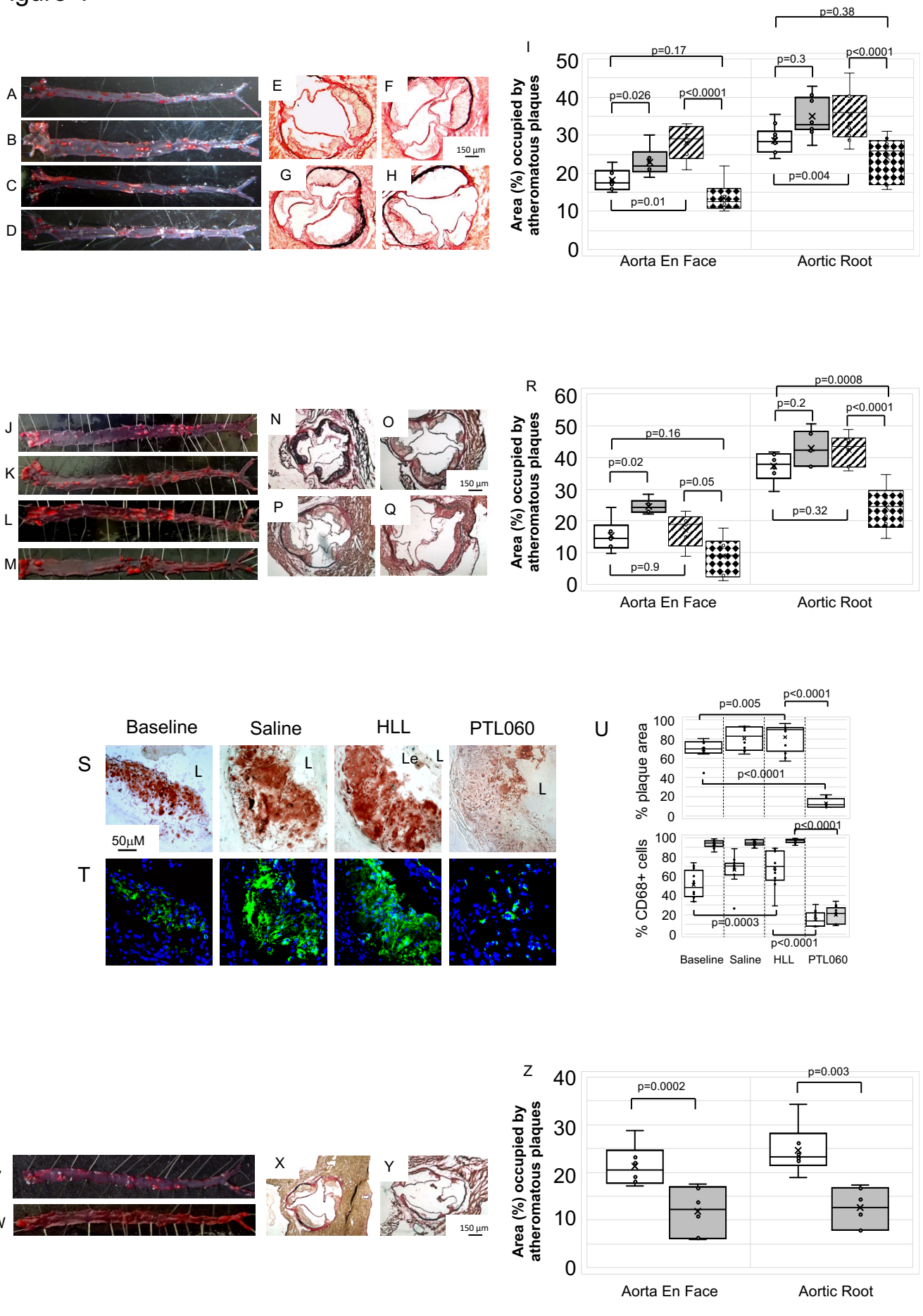
A
B
C
D
E
F
G
H
150 µm
I
Area (%) occupied by atheromatous plaques
p=0.38
p=0.17
p=0.3
p<0.0001
p=0.026
p<0.0001
p=0.004
p=0.01
Aorta En Face
Aortic Root
J
K
L
M
N
O
P
Q
150 µm
R
Area (%) occupied by atheromatous plaques
p=0.0008
p=0.2
p<0.0001
p=0.16
p=0.02
p=0.05
p=0.32
p=0.9
Aorta En Face
Aortic Root
Baseline
Saline
HLL
PTL060
S
L
Le
50µM
T
U
% plaque area
p=0.005
p<0.0001
p<0.0001
% CD68+ cells
p<0.0001
p=0.0003
p<0.0001
Baseline
Saline
HLL
PTL060
V
W
X
Y
150 µm
Z
Area (%) occupied by atheromatous plaques
p=0.0002
p=0.003
Aorta En Face
Aortic Root

Figure 4: IV PTL060 causes regression of atherosclerosis

A-D: Representative Oil Red O-stained en face preparations of aorta from ApoE-/- mice fed a HFD from age of 6-22 weeks (baseline: A), or 6-28 weeks with weekly injections (weeks 23-28) of saline (B), control cytotopic 'tail' compound (C) or PTL060 10μg/g (D).

E-H: Representative light photomicrographs of elastic/van Gieson stained sections from aortic root of ApoE-/- mice fed a HFD from age of 6-22 weeks (baseline: E), or 6-28 weeks with weekly injections (weeks 23-28) of saline (F), control cytotopic 'tail' compound (G) or PTL060 10μg/g (E).

I: Quantative comparison of impact of PTL060 on atheroma formation in mice on HFD aged 6-22 weeks (white bars) or 6-28 weeks with weekly injections (weeks 23-28) of saline (grey bars), control 'tail' compound (striped bars) or PTL060 10μg/g (diamond bars). Comparisons of plaque development analysed by repeated measures two way Anova. Because multiple comparisons were made from these animals, $p<0.008$ is statistically significant.

J-M: Representative Oil Red O-stained en face preparations of aorta from ApoE-/- mice fed a HFD from age of 6-22 weeks (Baseline: J), or 6-28 weeks with weekly injections (weeks 23-28) of saline (K), control 'untailed' HLL (L) or PTL060 10μg/g (M).

N-Q: Representative light photomicrographs of elastic/van Gieson stained sections from aortic root of ApoE-/- mice fed a HFD from age of 6-22 weeks (N), or 6-28 weeks with weekly injections (weeks 23-28) of saline (O), control untailed HLL (P) or PTL060 10μg/g (Q).

R: Quantative comparison of impact of PTL060 on atheroma formation in mice on HFD aged 6-22 weeks (white bars) followed by weekly injections, for 6 weeks of saline (grey bars), control untailed HLL (striped bars) or PTL060 10μg/g (diamond bars). Comparisons of plaque development analysed by repeated measures two way Anova. Because multiple comparisons were made from these animals, $p<0.0026$ is statistically significant.

S-T: Impact of PTL060 on foam cells in atherosclerosis. Representative light photomicrographs of elastic/van Gieson stained sections from aortic root (S) with consecutive sections analysed by two-colour immunofluorescence (T) stained with DAPI (blue) or anti-CD68 (green). ApoE-/- mice were fed a HFD from age of 6-22 weeks, followed by weekly injections, for 6 weeks of saline, control untailed HLL or PTL060 10μg/g as indicated.

U: Graphical representations of the % of plaque area staining with Oil Red O (upper panel) and, in lower panel, the % of area occupied by CD68+ cells (white bars) with the proportion of those CD68+ cells co-localising with lipid (grey bars). Each graph is a box plot with median with interquartile range (IQR) with whiskers showing upper and lower limits and outliers indicated as single data points. Means are represented with 'x'. Data is derived from an assessment of each of the three aortic root plaques from 6 individual mice, from consecutive sections as illustrated in S&T. Comparisons of plaque development analysed by repeated measures two way Anova. Because multiple comparisons were made from these animals, $p<0.0026$ is statistically significant.

V-W: Representative Oil Red O-stained en face preparations of aorta from ApoE-/- mice fed a normal chow diet to the age of 28 weeks, followed by weekly injections, for 6 weeks of saline (V) or PTL060 10μg/g (W).

X-Y: Representative light photomicrographs of elastic/van Gieson stained sections from aortic root of ApoE-/- mice fed a chow diet age to the age of 28 weeks, followed by weekly injections, for 6 weeks of saline (X) or PTL060 10μg/g (Y).

Z: Quantative comparison of impact of PTL060 on atheroma formation in mice on chow diet to for 28 weeks followed by weekly injections, for 6 weeks of saline (white bars) or PTL060 10μg/g (grey bars). Comparisons of plaque development analysed by two way Anova. $P<0.05$ is statistically significant.

Figure 5

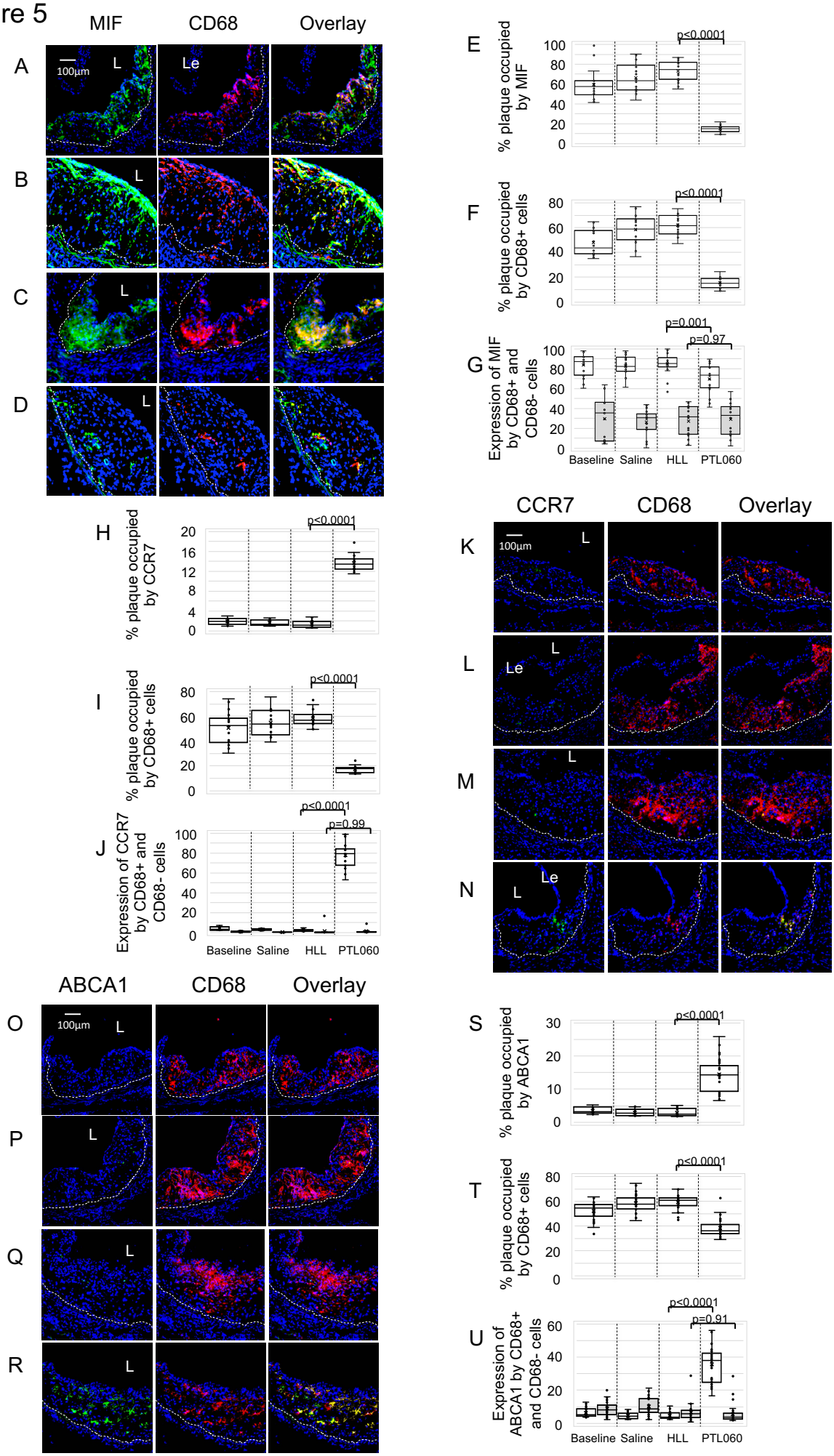
MIF
CD68
Overlay
A
B
C
D
100µm
L
Le
E
% plaque occupied by MIF
p<0.0001
F
% plaque occupied by CD68+ cells
p<0.0001
G
Expression of MIF by CD68+ and CD68- cells
p=0.001
p=0.97
Baseline
Saline
HLL
PTL060
H
% plaque occupied by CCR7
p<0.0001
I
% plaque occupied by CD68+ cells
p<0.0001
J
Expression of CCR7 by CD68+ and CD68- cells
p<0.0001
p=0.99
CCR7
CD68
Overlay
K
L
M
N
ABCA1
CD68
Overlay
O
P
Q
R
S
% plaque occupied by ABCA1
p<0.0001
T
% plaque occupied by CD68+ cells
p<0.0001
U
Expression of ABCA1 by CD68+ and CD68- cells
p<0.0001
p=0.91

Figure 5: Phenotype of plaque cells after PTL060

Three colour immunofluorescence images show confocal microscopic analysis of consecutive sections of aortic roots of ApoE-/- mice, fed a high fat diet from 6 to 22 weeks ('Baseline' A, K,O) or 6-28 weeks, with mice administered weekly injections of saline (B,L,P), HLL (C,M,Q), or PTL060 (D,N,R) as indicated between weeks 22-28. Panels show the plaque expression of CD68 (red) with (green) either MIF (A-D) CCR7 (K-N) or ABCA1 (O-R). Yellow in overlay image indicates co-localisation. The plaque area is demarcated by the lumen (L) and the dotted white line. Le= aortic leaflet.

Each panel of images is accompanied by graphical representations of the % of plaque area staining for the molecule of interest (E-MIF, H-CCR7, S-ABCA1) and the % of plaque area occupied by CD68+ (F, I, T) and the proportion of CD68+ cells (white bars) and CD68- negative cells (grey bars) co-staining for MIF (G), CCR7 (J), or ABCA1 (U). Each graph is a box plot with median with interquartile range (IQR) with whiskers showing upper and lower limits and outliers indicated as single data points. Means are represented with 'x'. Each is derived from an assessment of each of the three aortic root plaques from 6-24 individual mice.

Comparisons of plaque composition analysed by repeated measures two way Anova. Because multiple comparisons were made from these animals, $p<0.0026$ is statistically significant.

Figure 6

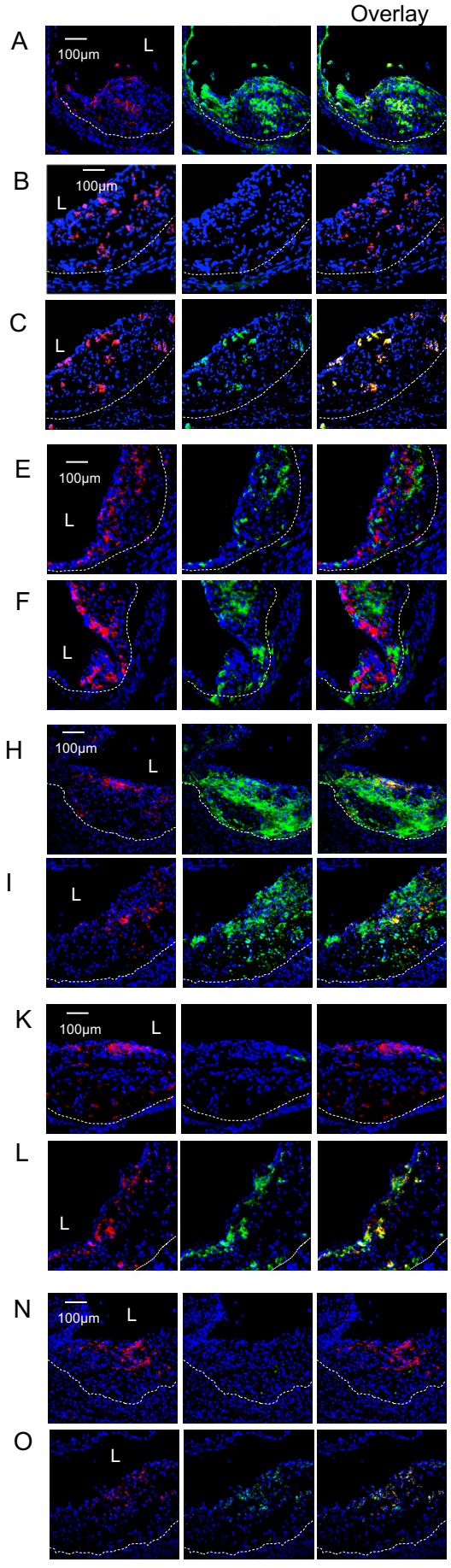
Overlay
A
B
C
E
F
H
I
K
L
N
O
100µm
L

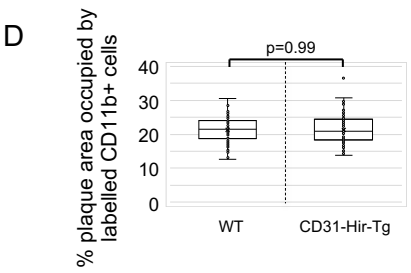
D
% plaque area occupied by labelled CD11b+ cells
p=0.99
40
30
20
10
0
WT
CD31-Hir-Tg

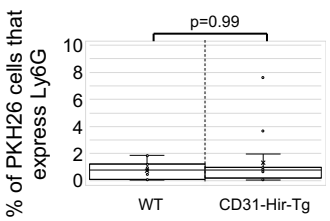
G
% of PKH26 cells that express Ly6G
p=0.99
10
8
6
4
2
0
WT
CD31-Hir-Tg

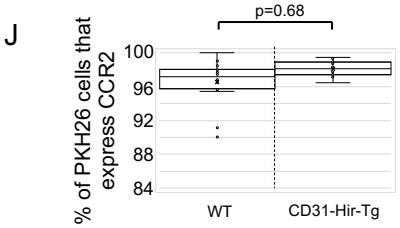
J
% of PKH26 cells that express CCR2
p=0.68
100
96
92
88
84
WT
CD31-Hir-Tg

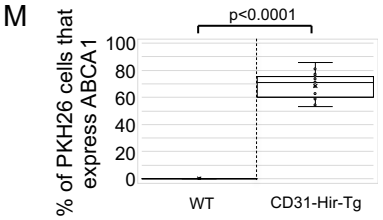
M
% of PKH26 cells that express ABCA1
p<0.0001
100
80
60
40
20
0
WT
CD31-Hir-Tg

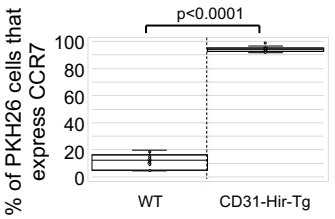
P
% of PKH26 cells that express CCR7
p<0.0001
100
80
60
40
20
0
WT
CD31-Hir-Tg

Figure 6 – Impact of adoptive transfer of CD11b+ cells expressing tethered thrombin inhibitor
All panels: CD11b cells, harvested from either BL/6 or CD31-Hir-Tg mice were labelled in vitro with PKH26 (red) and adoptively transferred into ApoE-/- mice fed a HFD between ages of 6-22 weeks. Aortic roots were collected 48 hours post-injection, for confocal IF analysis of the phenotype of adoptively transferred cells. Graphs are a box plot with median with interquartile range (IQR) with whiskers showing upper and lower limits and outliers indicated as single data points. Means are represented with 'x'. Each is derived from an assessment of at least 3 aortic root plaques from 6-35 individual mice.
A: To illustrate the expression of MIF (green) at baseline age 22 weeks, throughout the plaque area in a mouse that received BL/6 CD11b+ cells.
B-D: Comparison of the recruitment of CD11b+ cells from BL/6 (B) and CD31-Hir-Tg (C) mice. Hirudin (green) only seen in cells from CD31-Hir-Tg mice. D illustrates quantitative assessment of the proportion of plaque area occupied by PKH26+ cells.
E-G: To illustrate expression of Ly6G (green) within the plaque after adoptive transfer of CD11b+ cells from BL/6 (E) or CD31-HIr-Tg (F) mice. G illustrates quantitative assessment of the proportion of PKH26+ cells co-expressing Ly6G.
I-J: To illustrate expression of CCR2 (green) within the plaque after adoptive transfer of CD11b+ cells from BL/6 (H) or CD31-HIr-Tg (I) mice. J illustrates quantitative assessment of the proportion of PKH26+ cells co-expressing CCR2.
K-M: To illustrate expression of ABCA1 (green) within the plaque after adoptive transfer of CD11b+ cells from BL/6 (K) or CD31-HIr-Tg (L) mice. M illustrates quantitative assessment of the proportion of PKH26+ cells co-expressing ABCA1.
N-P: To illustrate expression of CCR7 (green) within the plaque after adoptive transfer of CD11b+ cells from BL/6 (N) or CD31-HIr-Tg (O) mice. P illustrates quantitative assessment of the proportion of PKH26+ cells co-expressing CCR7.
Quantitative comparisons analysed by repeated measures two way Anova. Because multiple comparisons were made from these animals, $p<0.0055$ is statistically significant.

Figure 7

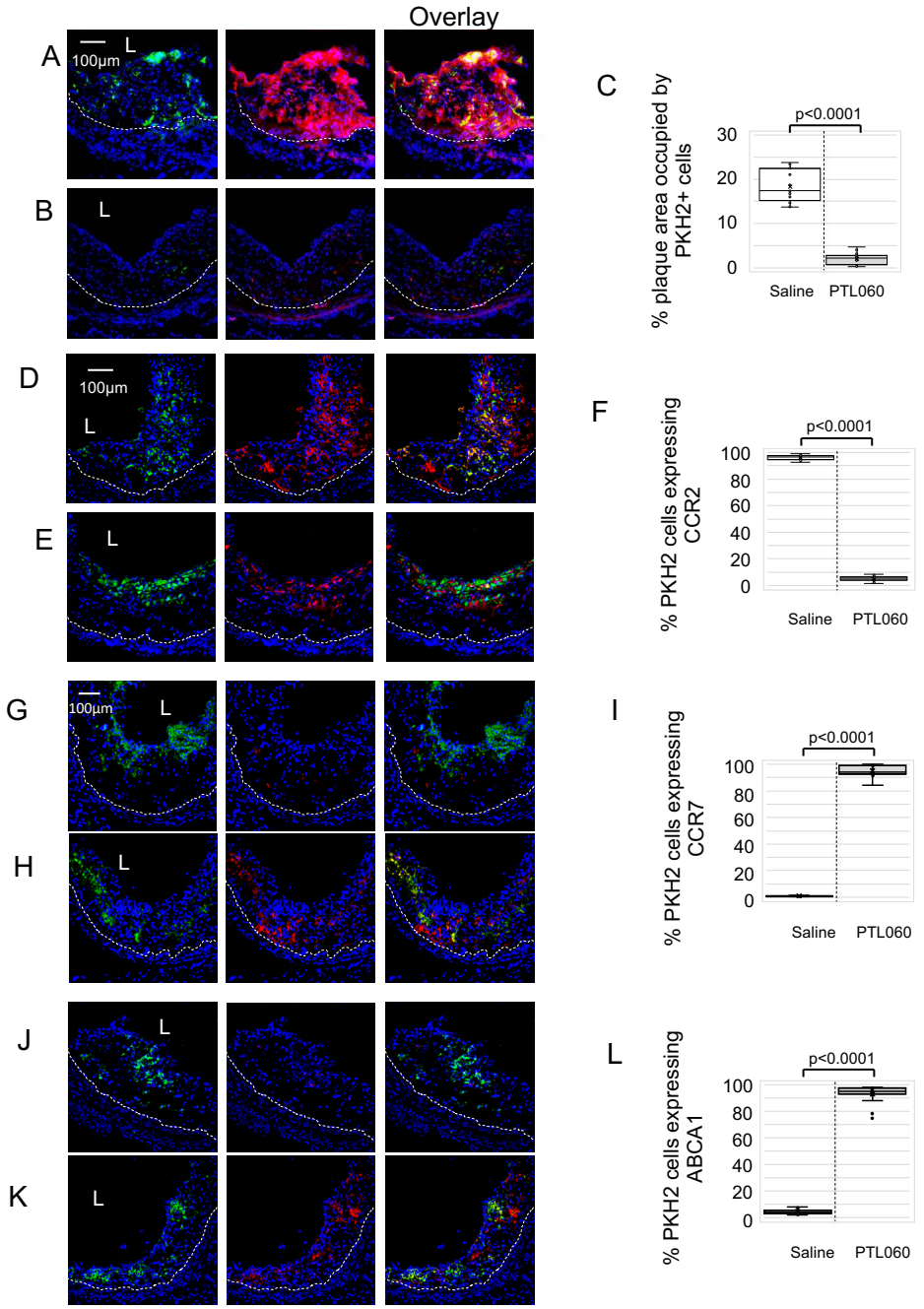
Overlay
A
100µm
L
B
L
C
p<0.0001
% plaque area occupied by PKH2+ cells
30
20
10
0
Saline
PTL060
D
100µm
L
E
L
F
p<0.0001
% PKH2 cells expressing CCR2
100
80
60
40
20
0
Saline
PTL060
G
100µm
L
H
L
I
p<0.0001
% PKH2 cells expressing CCR7
100
80
60
40
20
0
Saline
PTL060
J
L
K
L
L
p<0.0001
% PKH2 cells expressing ABCA1
100
80
60
40
20
0
Saline
PTL060

Figure 7: Monocyte recruitment and phenotype after systemic PTL060.
Confocal microscopic analysis of three colour immunofluorescence images through consecutive sections of aortic roots of ApoE-/- mice, fed a high fat diet from 6 to 26 weeks, with mice administered weekly injections of saline or PTL060 as indicated below between weeks 22-25. 1 week after the last injection, mice were injected with PKH2-labelled CD11b cells (green) and aortic roots harvested 48 hours later. Graphs are a box plot with median with interquartile range (IQR) with whiskers showing upper and lower limits and outliers indicated as single data points. Means are represented with 'x'. Each is derived from a double assessment of each of the three aortic root plaques from 3 individual mice.
A-C: To illustrate the expression of MIF (red) after adoptive transfer of BL/6 CD11b+ cells in mice treated with saline (A) or PTL060 (B). C illustrates quantitative assessment of the proportion of plaque area occupied by PKH2+ cells. D-F: To illustrate the expression of CCR2 (red) after adoptive transfer of BL/6 CD11b+ cells in mice treated with saline (D) or PTL060 (E). F illustrates quantitative assessment of the proportion of PKH2+ cells co-expressing CCR2. G-I: To illustrate the expression of CCR7 (red) after adoptive transfer of BL/6 CD11b+ cells in mice treated with saline (G) or PTL060 (H). I illustrates quantitative assessment of the proportion of PKH2+ cells co-expressing CCR7. J-K: To illustrate the expression of ABCA1 (red) after adoptive transfer of BL/6 CD11b+ cells in mice treated with saline (J) or PTL060 (K). L illustrates quantitative assessment of the proportion of PKH2+ cells co-expressing ABCA1. Quantitative comparisons analysed by repeated measures two way Anova. Because multiple comparisons were made from these animals, $p<0.007$ is statistically significant

Figure 8

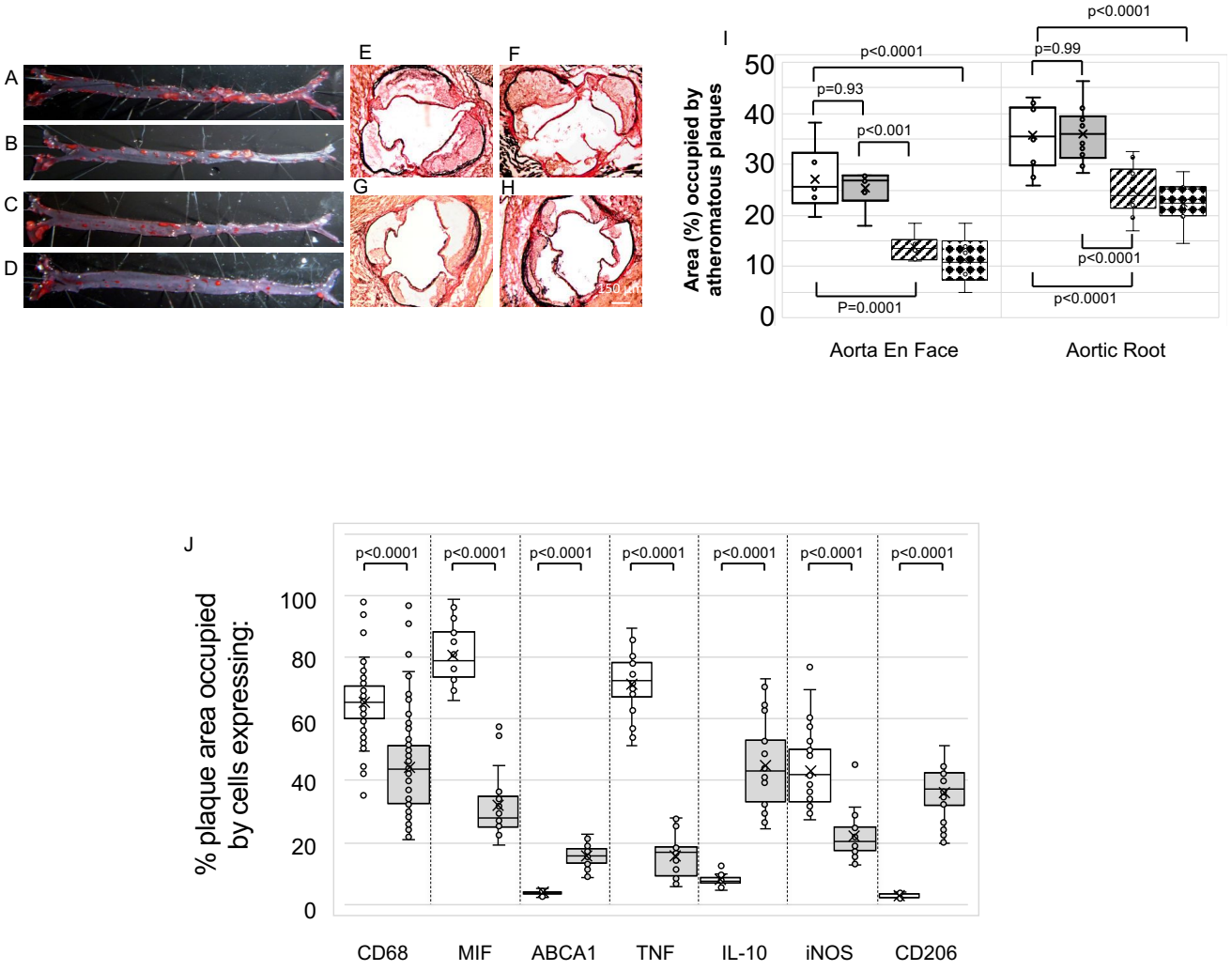

Figure 8: *Regression induced by thrombin inhibitor on isolated CD11b+ cells*
Samples represented here are from ApoE-/- mice fed a HFD from age of 6-28 weeks with weekly (weeks 23-28) injections of CD11b+ cells from BL/6 mice pre-incubated with saline (A, E), control 'tail' molecule (B, F), PTL060 100μM (C,G) or with CD11b cells from CD31-Hir-Tg mice (D, H)
A-D: Representative Oil Red O-stained en face preparations of aorta
E-H: Representative light photomicrographs of elastic/van Gieson stained sections from aortic root
I: Quantitative comparison of atheroma regression in the whole aorta (en face) or aortic root of mice fed a HFD from age of 6-28 weeks with weekly (weeks 23-28) injections of CD11b+ cells from BL/6 mice pre-incubated with saline (white bars), control 'tail' molecule (grey bars), PTL060 100μM (striped bars) or with CD11b cells from CD31-Hir-Tg mice (diamond bars).
J: Graph is a box plot with median with interquartile range (IQR) with whiskers showing upper and lower limits and outliers indicated as single data points. Means are represented with 'x'. Each is derived from an assessment of at least 3 aortic root plaques from 6-24 individual mice. It illustrates the proportion of plaque area occupied by cells expressing the various markers (as indicated on abscissa) from mice receiving CD11b+ cells from BL/6 mice pre-incubated with saline (white bars) or CD31-Hir-Tg mice (grey bars).
Quantitative comparisons in I&J analysed by repeated measures two way Anova. Because multiple comparisons were made from these animals, $p<0.0055$ is statistically significant.

Supplemental Material

Supplementary Table 1
% viability within Macrophage Forward Scatter / Side scatter gate, as assessed by LIVE /Dead aqua fluorescent dye.
See methods for details

	Incubation time (minutes)		
	30	60	120
Control PBS	-	-	99
25μM PTL060	99	95	96
50 μM PTL060	96	98	92
100 μM PTL060	97	87	80

Supplementary Table 2
Viability of adoptively transferred CD11b cells, assessed by trypan blue exclusion, after incubation with saline, control tail only peptides (100μM), or PTL060 (100μM) for 30 minutes immediately prior to injection.

	Incubated with		
	Saline	Control tail peptides only	PTL060
Mean % viability	97.1	97.1	97.2
SEM	0.16	0.1	0.16

Supplementary Figure 1

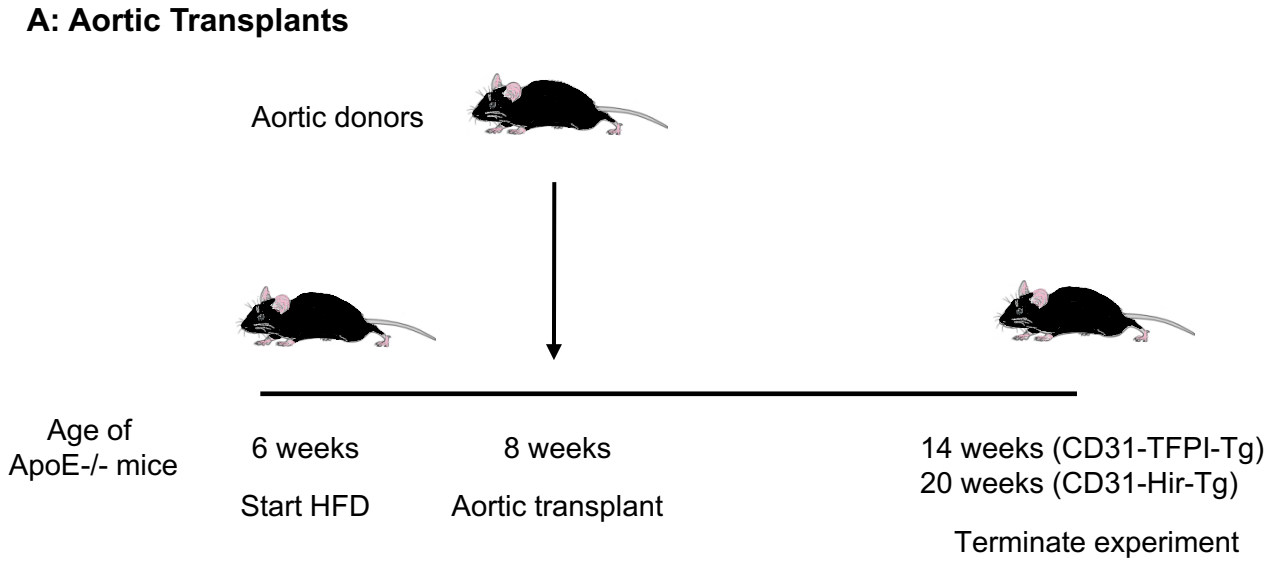

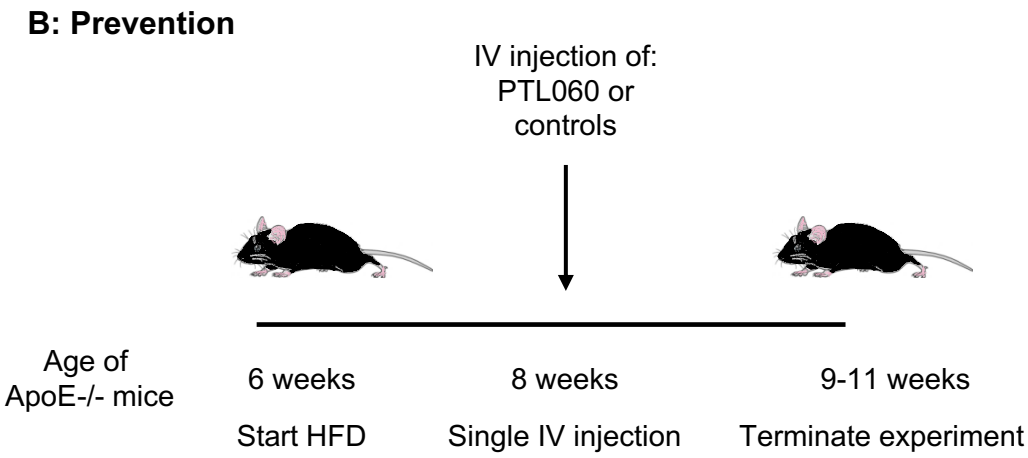

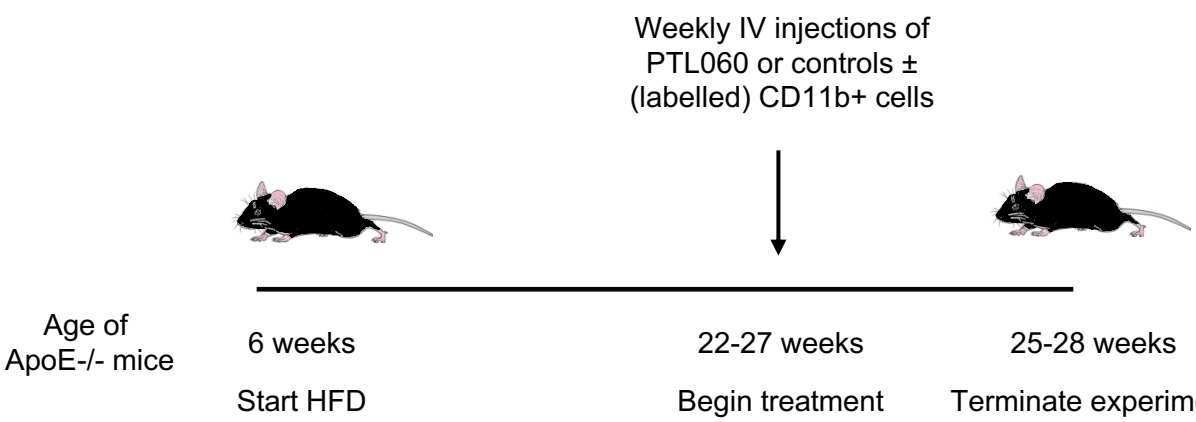

Supplementary Figure 2

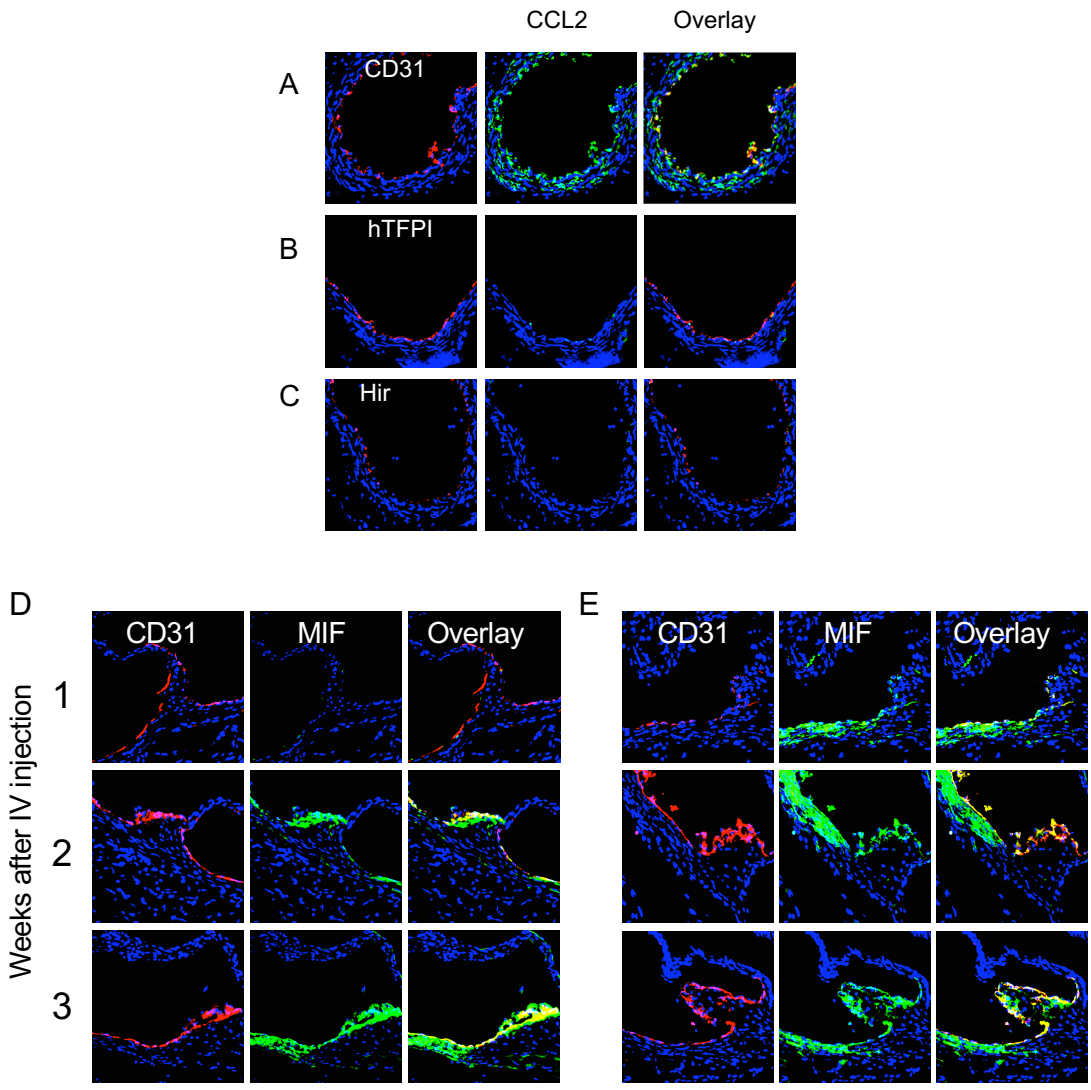

Suppl Figure 2: Inhibition of TF or thrombin on EC abolishes CCL2 and MIF expression in vascular walls

A-C. Three colour immunofluorescence images of sections through donor aortas, 6 weeks post-transplantation. Recipients were ApoE-/- mice, fed a high fat diet (HFD) for two weeks from age 6 weeks, prior to transplantation of aorta from BL/6 (A) CD31-TFPI-Tg (B) or CD31-Hir-Tg (C). Blue - nuclear stain 4',6-diamidino-2-phenylindole (DAPI). Red - anti-CD31 (A) anti-hTFPI (B) or anti-hirudin (Hir-C). Green – CCL2. Each panel of three images shows consecutive sections.

D&E: Three colour IF images of consecutive sections through aortic root, taken 1, 2 or 3 weeks post IV injection of 10μg/g of PTL060 (D) or PBS (E). ApoE-/- mice were commenced on a high fat diet 2 weeks prior to the injections. Blue - DAPI. Red - anti-CD31. Green - MIF.

Supplementary Figure 3

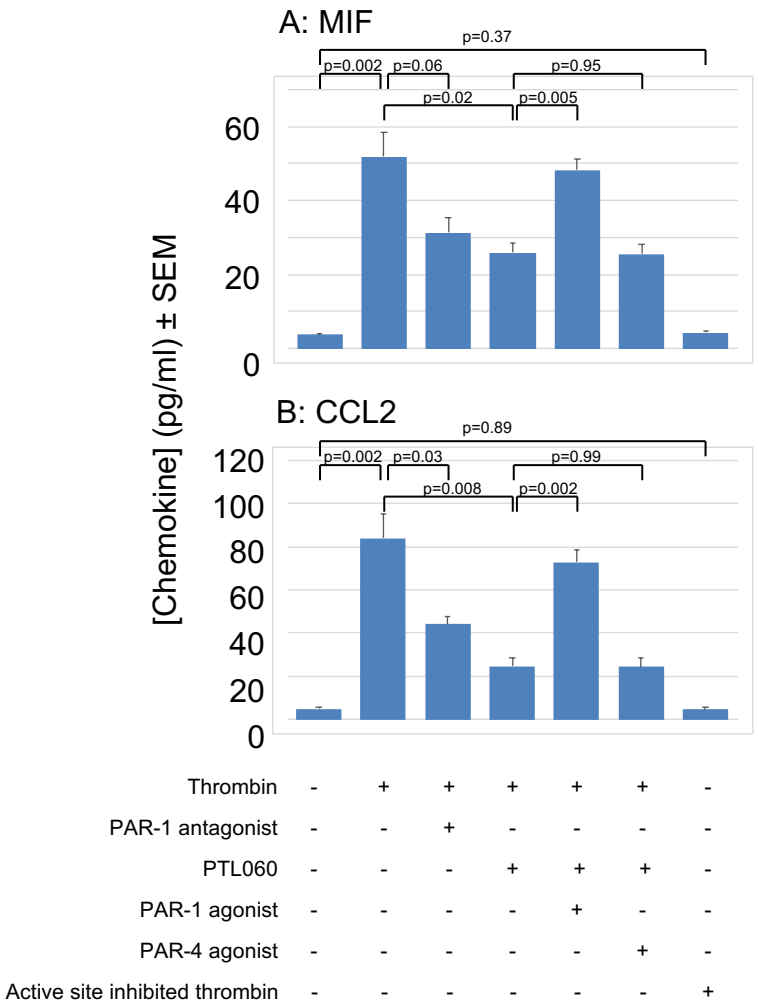

Suppl Figure 3: PTL060 inhibits thrombin- and PAR-1-mediated chemokine production in vitro.

In vitro analysis of MIF (A) or CCL2 (B) production by cultured mouse SMCs, following stimulation by thrombin, with addition of reagents to demonstrate that PTL060 predominantly inhibits PAR-1 mediated chemokine production. N=3 measures per sample. Comparisons of significance by unpaired 2-tailed students t test. $P<0.05$ is considered significant.

Experiment repeated twice.

Supplementary Figure 4

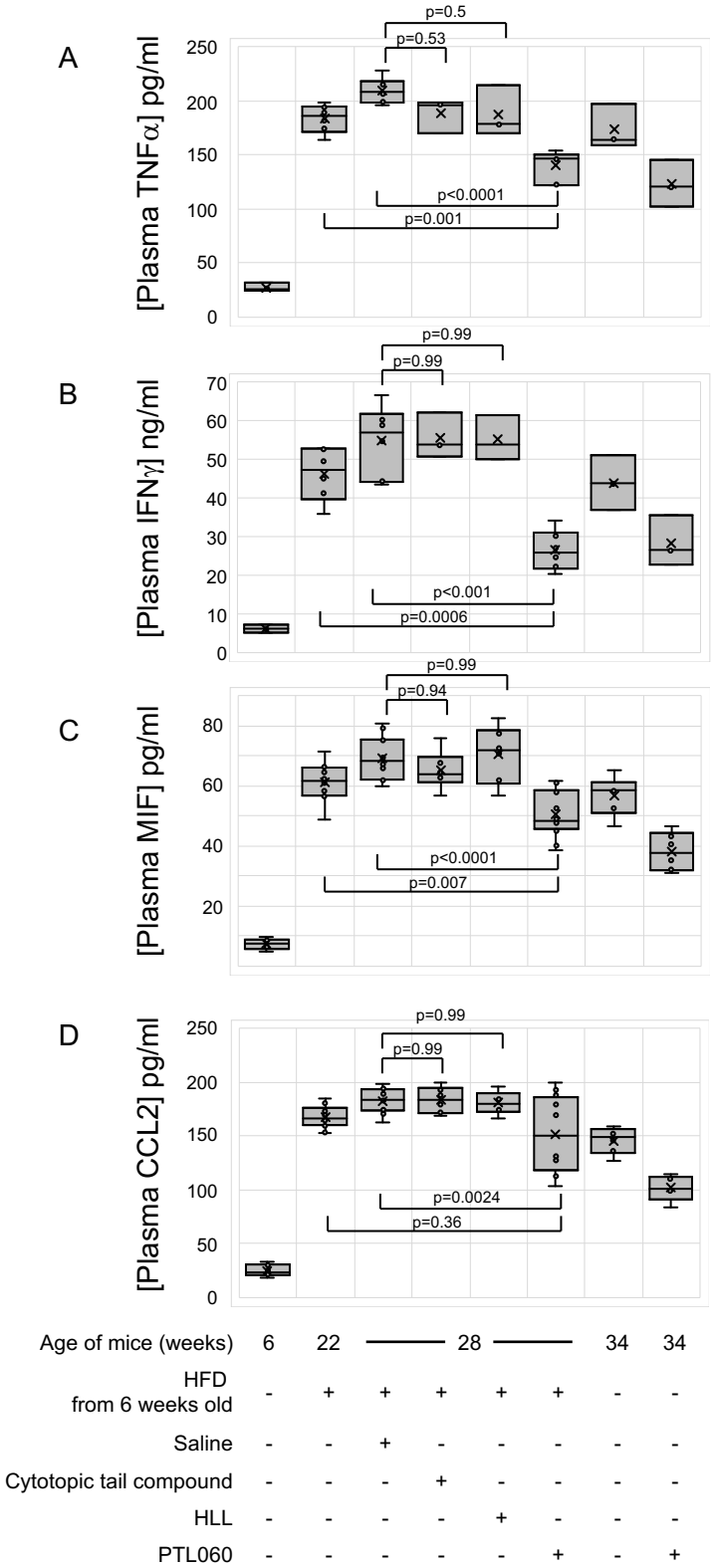

Suppl Figure 4: Systemic inhibition of inflammation by PTL060.
Plasma TNFα (A), IFNγ (B), MIF (C) and CCL2 (D) in different groups of ApoE-/- mice, as indicated on abscissa.
Graphs show box plots with median with interquartile range (IQR) with whiskers showing upper and lower limits and outliers indicated as single data points. Means are represented with 'x'. Comparisons analysed by repeated measures two way Anova. Because multiple comparisons were made from these animals, $p<0.0026$ is statistically significant.

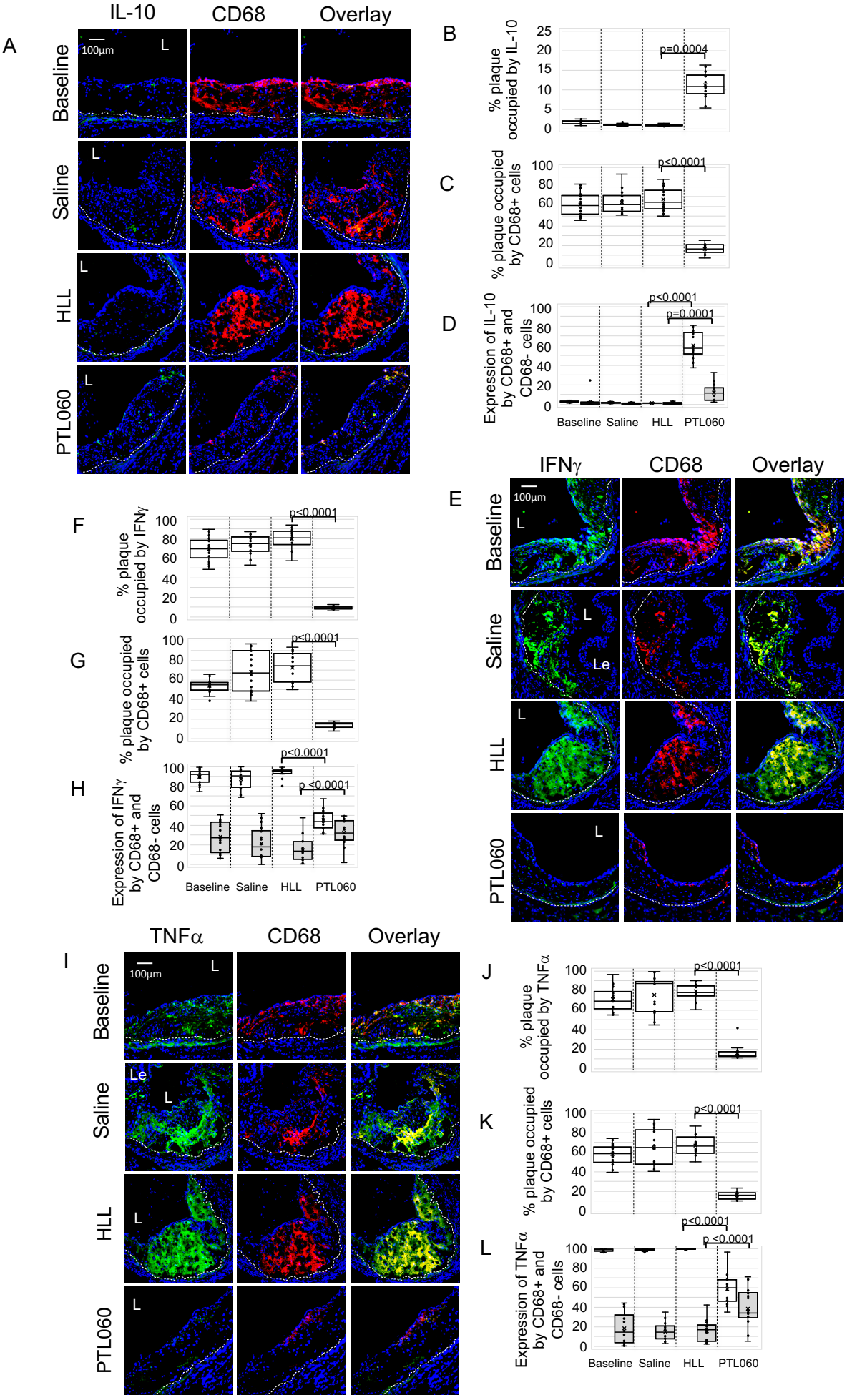
A
IL-10
CD68
Overlay
100µm
L
Baseline
Saline
HLL
PTL060
B
% plaque occupied by IL-10
p=0.0004
C
% plaque occupied by CD68+ cells
p<0.0001
D
Expression of IL-10 by CD68+ and CD68- cells
p<0.0001
p=0.0001
Baseline Saline HLL PTL060
E
IFNγ
CD68
Overlay
Le
F
% plaque occupied by IFNγ
p<0.0001
G
% plaque occupied by CD68+ cells
p<0.0001
H
Expression of IFNγ by CD68+ and CD68- cells
p<0.0001
p <0.0001
Baseline Saline HLL PTL060
I
TNFα
CD68
Overlay
J
% plaque occupied by TNFα
p<0.0001
K
% plaque occupied by CD68+ cells
p<0.0001
L
Expression of TNFα by CD68+ and CD68- cells
p<0.0001
p <0.0001
Baseline Saline HLL PTL060

Suppl Figure 5: Phenotype of plaque cells induced by PTL060_2

Confocal microscopic analysis of three colour immunofluorescence images through consecutive sections of aortic roots of ApoE-/- mice, fed a high fat diet from 6 to 22 weeks ('Baseline', all panels) or 6-28 weeks, with mice administered weekly injections of saline, HLL, or PTL060 as indicated between weeks 22-28. Panels show the plaque expression of CD68 (red) with (green) either IL-10 (A) IFNγ (E) or TNFα (I). Yellow in overlay image indicates co-localisation. The plaque area is demarcated by the lumen (L) and the dotted white line. Le= aortic leaflet.

Each panel of images is accompanied by graphical representations of the % of plaque area staining for the molecule of interest (B-IL-10, F-IFNγ, J-TNF α) and the % of plaque area occupied by CD68+ (C, G, K) and the proportion of CD68+ cells (white bars) and CD68-negative cells (grey bars) co-staining for IL-10 (D), IFNγ (H), or TNF α (L). Each graph is a box plot with median with interquartile range (IQR) with whiskers showing upper and lower limits and outliers indicated as single data points. Means are represented with 'x'. Each is derived from an assessment of each of the three aortic root plaques from at least 6 individual mice. Comparisons analysed by repeated measures two way Anova. Because multiple comparisons were made from these animals, $p<0.0026$ is statistically significant.

Supplementary figure 6

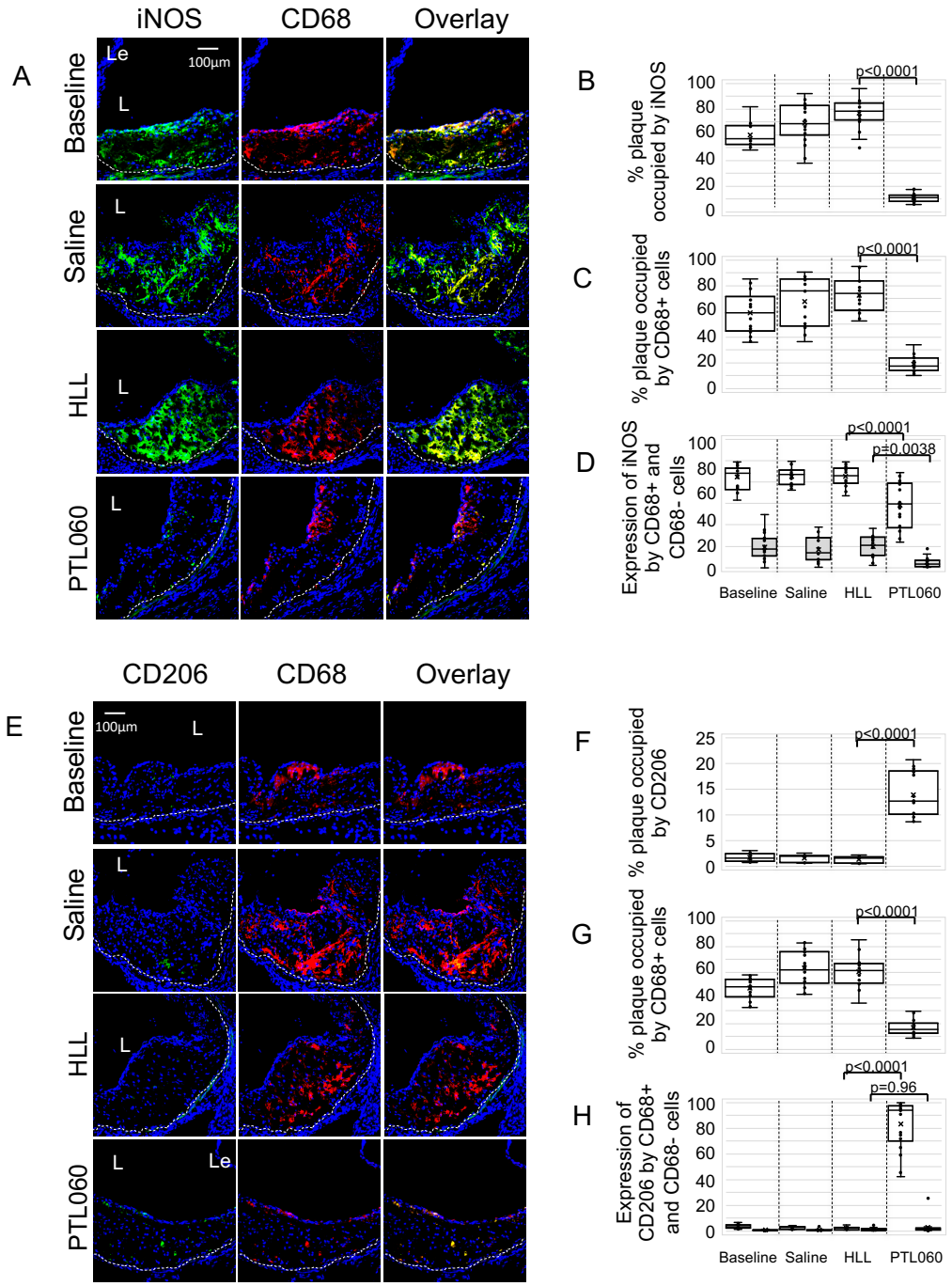

Figure 6: Phenotype of plaque cells induced by PTL060_3

Confocal microscopic analysis of three colour immunofluorescence images through consecutive sections of aortic roots of ApoE-/- mice, fed a high fat diet from 6 to 22 weeks ('Baseline', all panels) or 6-28 weeks, with mice administered weekly injections of saline, HLL, or PTL060 as indicated between weeks 22-28. Panels show the plaque expression of CD68 (red) with (green) either iNOs (A) or CD206 (E). Yellow in overlay image indicates co-localisation. The plaque area is demarcated by the lumen (L) and the dotted white line. Le= aortic leaflet.

Each panel of images is accompanied by graphical representations of the % of plaque area staining for the molecule of interest (B-iNOS, F-CD206) and the % of plaque area occupied by CD68+ (C, G) and the proportion of CD68+ cells (white bars) and CD68-negative cells (grey bars) co-staining for iNOS (D) or CD206 (H). Each graph is a box plot with median with interquartile range (IQR) with whiskers showing upper and lower limits and outliers indicated as single data points. Means are represented with 'x'. Each is derived from an assessment of each of the three aortic root plaques from at least 6 individual mice. Comparisons analysed by repeated measures two way Anova. Because multiple comparisons were made from these animals, p<0.0026 is statistically significant.

Supplementary figure 7

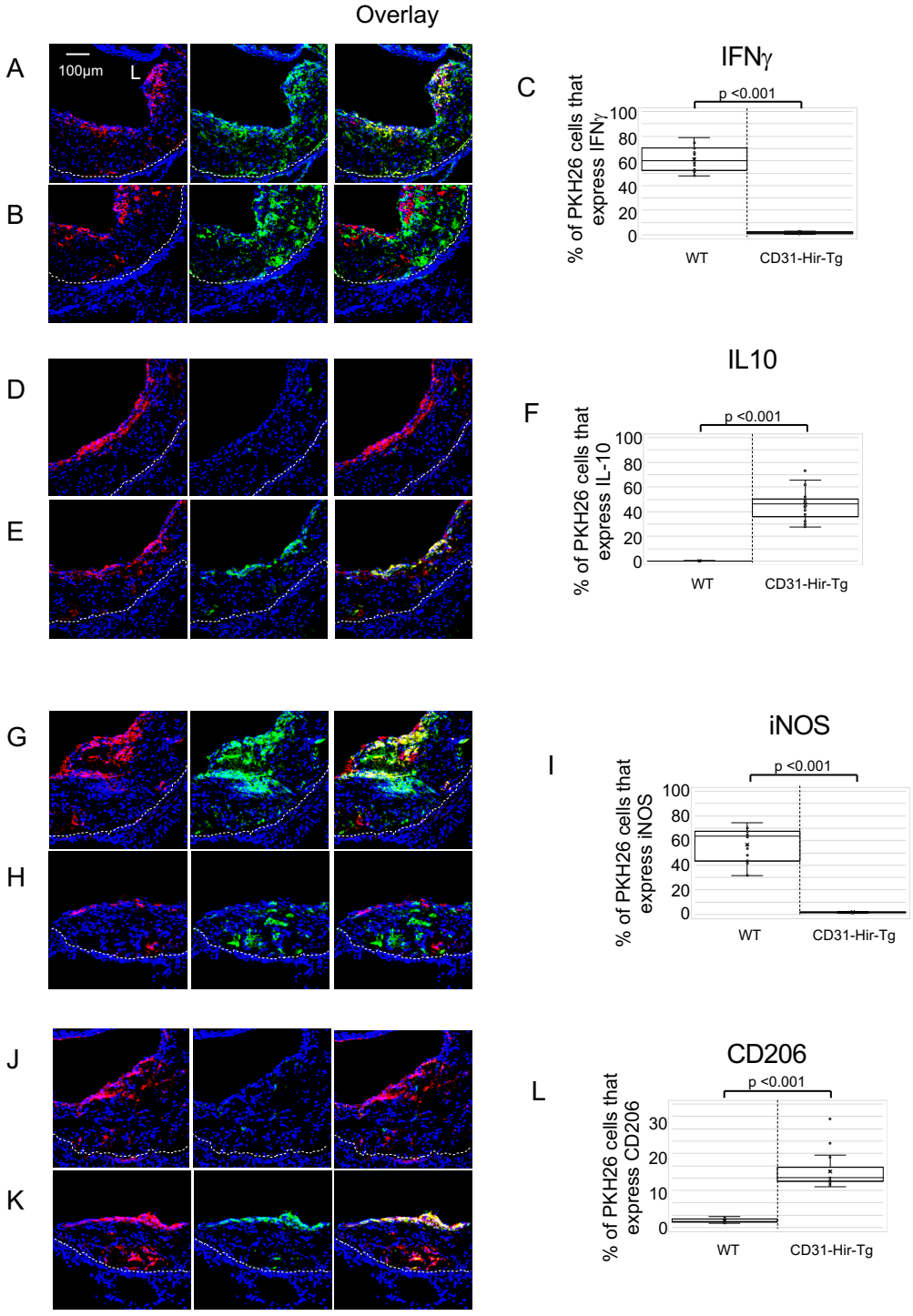

Figure 7 – Impact of adoptive transfer of CD11b+ cells expressing hirudin_2
All panels: CD11b cells, harvested from either BL/6 or CD31-Hir-Tg mice were labelled in vitro with PKH26 (red) and adoptively transferred into ApoE-/- mice fed a HFD between ages of 6-22 weeks. Aortic roots were collected 48 hours post-injection, for confocal IF analysis of the phenotype of adoptively transferred cells. Graphs are a box plot with median with interquartile range (IQR) with whiskers showing upper and lower limits and outliers indicated as single data points. Means are represented with 'x'. Each is derived from a double assessment of each of the six aortic root plaques from 6 individual mice.
A-C: To illustrate expression of IFNγ (green) within the plaque after adoptive transfer of CD11b+ cells from BL/6 (A) or CD31-HIr-Tg (B) mice. (C) illustrates quantitative assessment of the proportion of PKH26+ cells co-expressing IFNγ .
D-F: To illustrate expression of IL-10 (green) within the plaque after adoptive transfer of CD11b+ cells from BL/6 (D) or CD31-HIr-Tg (E) mice. (F) illustrates quantitative assessment of the proportion of PKH26+ cells co-expressing IL-10.
G-I: To illustrate expression of iNOS (green) within the plaque after adoptive transfer of CD11b+ cells from BL/6 (G) or CD31-HIr-Tg (H) mice. (I) illustrates quantitative assessment of the proportion of PKH26+ cells co-expressing iNOS.
J-L: To illustrate expression of CD206 (green) within the plaque after adoptive transfer of CD11b+ cells from BL/6 (J) or CD31-HIr-Tg (K) mice. (L) illustrates quantitative assessment of the proportion of PKH26+ cells co-expressing CD206.
Quantitative comparisons analysed by repeated measures two way Anova. Because multiple comparisons were made from these animals, $p<0.0055$ is statistically significant.

Supplementary Figure 8

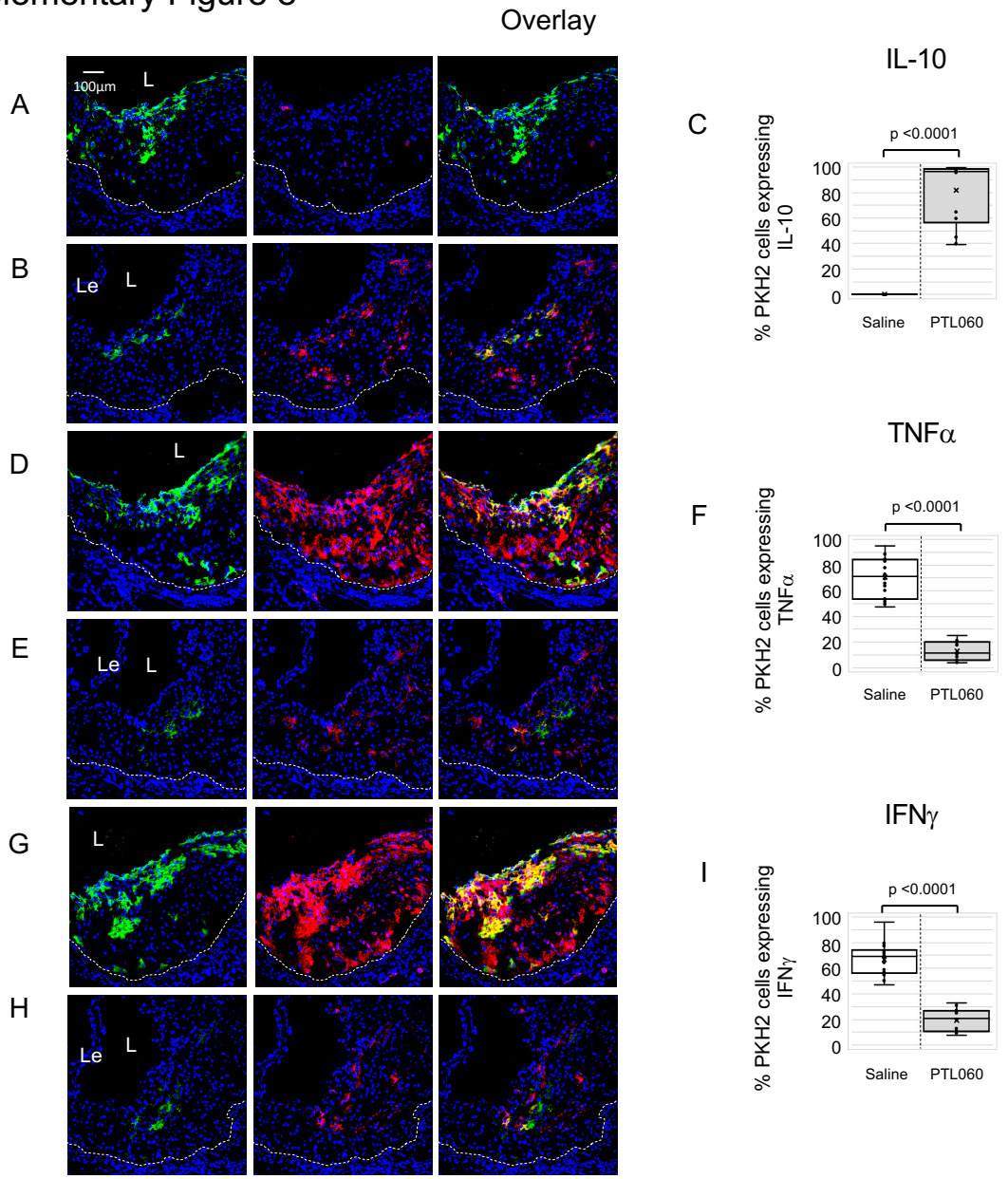

Figure 8: Monocyte recruitment and phenotype after systemic PTL060_2.
Confocal microscopic analysis of three colour immunofluorescence images through consecutive sections of aortic roots of ApoE-/- mice, fed a high fat diet from 6 to 26 weeks, with mice administered weekly injections of saline or PTL060 as indicated below between weeks 22-25. 1 week after the last injection, mice were injected with PKH2-labelled CD11b cells (green) and aortic roots harvested 48 hours later. Graphs are a box plot with median with interquartile range (IQR) with whiskers showing upper and lower limits and outliers indicated as single data points. Means are represented with 'x'. Each is derived from a double assessment of each of the three aortic root plaques from 3 individual mice.

A-C: To illustrate the expression of IL-10 (red) after adoptive transfer of BL/6 CD11b+ cells in mice treated with saline (A) or PTL060 (B). (C) illustrates quantitative assessment of the proportion of PKH2+ cells co-expressing IL-10.

D-F: To illustrate the expression of TNFα (red) after adoptive transfer of BL/6 CD11b+ cells in mice treated with saline (D) or PTL060 (E). (F) illustrates quantitative assessment of the proportion of PKH2+ cells co-expressing TNFα.

G-I: To illustrate the expression of IFNγ (red) after adoptive transfer of BL/6 CD11b+ cells in mice treated with saline (G) or PTL060 (H). (I) illustrates quantitative assessment of the proportion of PKH2+ cells co-expressing IFNγ.

Quantitative comparisons analysed by repeated measures two way Anova. Because multiple comparisons were made from these animals, $p<0.007$ is statistically significant.